Journal of Molecular Spectroscopy **214,** 152–174 (2002)
doi:10.1006/jmsp.2002.8567

High-Resolution Survey of the Visible Spectrum of NiF by Fourier Transform Spectroscopy

Y. Krouti,* T. Hirao,‡,[1] C. Dufour,† A. Boulezhar,* B. Pinchemel,†,[2] and P. F. Bernath‡

**Laboratoire de Physique Atomique et Moléculaire, Faculté des Sciences Aïn Chock B.P., 5366 Maârif, Casablanca, Morocco; †Laboratoire de Physique des Lasers, Atomes et Molécules, UMR CNRS 8523, Centre d'Etudes et de Recherches Laser et Applications, Université de Lille I 59655, Villeneuve d'Ascq Cedex, France; and ‡Department of Chemistry, University of Waterloo, Waterloo, Ontario, Canada N2L 3G1*

Received January 25, 2002; in revised form April 11, 2002

High-resolution spectra of NiF have been recorded in emission by Fourier transform spectroscopy using a very stable discharge source. The 0–0 bands of 14 electronic transitions have been studied, 6 of them for the first time. This work confirms the presence of 5 low-lying spin components $X^2\Pi_{3/2}$, $[0.25]^2\Sigma^+$, $[0.83]A^2\Delta_{5/2}$, $[1.5]B^2\Sigma^+$, and $[2.2]A^2\Delta_{3/2}$ as known from previous laser-induced fluorescence experiments. Eight electronic states are now identified in the 18 000–24 000 cm^{-1} range above the ground $X^2\Pi_{3/2}$ state. Electronic assignments for these excited states are not always obvious because of violations of the selection rules and unusual fine structure parameters. We think that some of the upper states are spin components of quartet states. In such a congested spectrum, high-resolution spectra are best analyzed in conjunction with an energy level diagram constructed mainly by dispersed low resolution laser-induced fluorescence.

I. INTRODUCTION

Numerous papers have been devoted to the study of the electronic structure of NiF. The first studies were concerned with low-resolution (*1–3*) and high-resolution (*4–10*) emission spectra. They showed that several low-lying states are involved in the observed transitions, but the nature of these states remained undetermined for a long time. For example, in one study the symmetry of the upper and lower states was switched (*4*), although the analysis of the rotational structure was correct. Bai and Hilborn (*11*) performed the first low-resolution study of dispersed laser-induced fluorescence of some of the rotationally analyzed bands in the blue-violet spectral region. They determined the relative position of two low-lying states, which were later revealed to be the $[0.83]A^2\Delta_{5/2}$ spin–orbit component and the $[1.5]B^2\Sigma^+$ state. At that time these two states had been suggested as possible ground states of NiF.

Experimental progress provided new information. High-resolution spectra of bands observed in the yellow-green spectral region were recorded and analyzed along with low-resolution dispersed laser-induced fluorescence (*6*). Simultaneously Carette *et al.* (*12*) proposed a theoretical energy level diagram based on ligand field theory. These studies supplied the first identification of the $X^2\Pi_{3/2}$ ground state and provided a credible assignment of the doublet electronic states of NiF located in the first 2500 cm^{-1} of the energy level diagram. Although the rotational and fine structure parameters of the $X^2\Pi_{3/2}$, $[0.83]A^2\Delta_{5/2}$, $[1.5]B^2\Sigma^+$, and $[2.2]A^2\Delta_{3/2}$ states were determined, the $X^2\Pi_{1/2}$ has not been identified yet, although there is a low-lying state located at 251 cm^{-1} above the $X^2\Pi_{3/2}$ state linked to several upper electronic states by dispersed laser-induced fluorescence experiments (*7–9*). The first analysis of a band involving this state was attempted by Dufour and Pinchemel (*9*), who studied the laser-induced fluorescence of a blue band located at 22 703 cm^{-1}. The $[22.9]^2\Pi_{3/2}$ upper state was well known (*7*) and the structure of this band has been interpreted as a $[22.9]^2\Pi_{3/2}$–$[0.25]^2\Sigma^+$ transition rather than the expected $^2\Pi_{3/2}$–$^2\Pi_{1/2}$ transition. We note that numerous forbidden transitions are observed in the spectrum of NiF. The most striking point of the analysis was that the spin–rotation parameter of the lower state, $\gamma = -0.952(1)$ cm^{-1}, was 2.5 times the value of the rotational constant, $B = 0.39009(5)$ cm^{-1}.

In a recent work Tanimoto *et al.* (*13*) published an experimental study of the rotational structure of the two lowest states of NiF ($X^2\Pi_{3/2}$ and $[0.25]^2\Sigma$ states) in the microwave spectral range. Following our analysis, Tanimoto *et al.* (*13*) described the electronic state located at 251 cm^{-1} as a $^2\Sigma$ state. Their work confirms our previous analysis (*9*) and they derived a spin–rotation constant $\gamma = -0.959722(2)$ cm^{-1} and a rotational parameter $B = 0.39001617(4)$ cm^{-1}. Carette *et al.* (*12*) showed that the first excited electronic state of NiF is a mixture of two states $[0.67\ ^2\Pi_{1/2} + 0.33\ ^2\Sigma]$. In addition, the rotational constants of the $X^2\Pi_{3/2}$ state ($B \approx 0.3886$ cm^{-1}) and $[0.25]^2\Sigma$ states ($B \approx 0.3900$ cm^{-1}) are significantly different although the rotational parameters of the two spin–orbit components of an electronic state are generally quite similar as observed, for example, for the $A^2\Delta_i$ state. As a consequence the description as a $^2\Sigma$ or

[1] Present address: Institute for Astrophysics and Planetary Sciences, Ibaraki University, 2-1-1 Bunkyo, Mito, Ibaraki, 310-8512, Japan.
[2] To whom correspondence should be addressed. E-mail: bernard.pinchemel@univ-lille1.fr.

as a $^2\Pi_{1/2}$ state is not appropriate and should be replaced by a $[0.25]\Omega = 1/2$ labeling because of the Hund's case (c) behavior. However, for sake of clarity we will keep the $[0.25]^2\Sigma$ labeling in this paper. The two spin–orbit components $[0.83]A^2\Delta_{5/2}$ and $[2.2]A^2\Delta_{3/2}$ of the $A^2\Delta_i$ state are also well known thanks to the analyses of bands recorded by high-resolution laser-excitation spectroscopy (*6, 7*), which provides an accurate determination of the wavenumbers of the lines. The $[1.5]B^2\Sigma^+$ state, however, is involved in transitions recorded at moderate resolution either with a grating spectrograph (*5*) or by dispersed laser-induced fluorescence using a grating spectrometer (*8*).

In Refs. (*4–9*), five upper electronic states have been identified and studied in several transitions involving the lower electronic states. A second set of transitions has also been observed (*10*) between a common upper state and five lower electronic components, which were not known.

Very recently Chen *et al.* (*14*) developed a molecular beam apparatus to study NiF by pulsed-dye laser excitation spectroscopy. The low temperature of the source (less than 100 K) selected only transitions involving the $X^2\Pi_{3/2}$ and the $[0.25]^2\Sigma^+$ states. In a second paper (*15*), Jin *et al.* analyzed eight transitions and they identified two new upper electronic states located at 20 282 cm^{-1} and 20 407 cm^{-1} in the energy level diagram. A third paper devoted to NiF has been recently published by Jin *et al.* (*16*), who studied most of the bands that we present in our paper. In the discussion section we compare our results with those of Jin *et al.* (*16*).

Up to now the most common technique used to study NiF has been emission spectroscopy using a hollow cathode (*4, 5*) or a microwave discharge (*6*) with a grating spectrometer utilized to disperse the light. Some spectra have been recorded by excitation spectroscopy in a Broida oven (*7*) using a single-mode dye laser. In addition, dispersed laser-induced fluorescence experiments with a grating spectrometer have been successful (*8–10*) and led to the measurement of the very large spin rotation parameter in the $[0.25]^2\Sigma^+$ electronic state. These diverse experiments provided several sets of constants for the same electronic state, and as already noted, the energy level diagrams associated with the different experiments were not always consistent. Consequently it was of interest to unify this patchwork of data. For this purpose we recorded the spectrum of NiF over the entire visible spectral range by using a high-resolution Fourier transform spectrometer and a very stable emission source. Under these experimental conditions we have reanalyzed most of the already known transitions. In addition, six new electronic transitions have been studied and a new electronic state (20 106 cm^{-1}) identified. For all transitions in which the $X^2\Pi_{3/2}$ and the $[0.25]^2\Sigma^+$ states are involved, the experimental microwave data published by Tanimoto *et al.* (*13*) have been added to the fits.

II. EXPERIMENTAL DETAILS

The emission spectra were recorded with the Bruker IFS 120HR Fourier transform spectrometer at the University of Waterloo (*17*). The spectrometer was equipped with a visible quartz beamsplitter and a pair of red and blue pass filters (450-nm red pass and 600-nm blue pass filters from CORION) were used to limit the spectral interval and to block the internal He–Ne laser to improve the signal-to-noise ratio. In total 285 scans at the resolution of 0.05 cm^{-1} were accumulated for the spectral region between 450 and 600 nm. Because the spectrometer was not evacuated during the measurement, the recorded spectral line positions have to be converted to vacuum wavenumbers (*17*). Electronically excited NiF molecules were generated by a D.C. discharge (3000 V, 0.3 A) in a 1-meter-long alumina tube (5 cm diameter), whose central part (50 cm) was externally heated to 930°C. A few grams of NiF_2 powder was introduced in the middle of the tube and a slow flow of argon maintained a pressure of 5 Torr. An intense blue-white discharge, whose stability was quite sensitive to the partial pressure of NiF_2, was observed. A 50-cm focal length lens focused the emitted light on the entrance aperture of the spectrometer. After the air-vacuum correction (*17*), the calibration was carried out by comparison of standard Ar I atomic lines (*18*) with the lines observed in our experiments. The calibration factor was 1.000001170 (11).

One of the previously studied bands (at 17 759 cm^{-1}) has been recorded by laser excitation spectroscopy (*7*) in Lille. This band was too weak to be identified in the emission spectra, but was easily observed by laser excitation. Note that the energy level diagram (Fig. 1) has been drawn on the basis of low-resolution of dispersed laser-induced fluorescence. No contradiction has been observed between these laser experiments and the rotational analysis of the bands described hereafter.

III. DESCRIPTION OF THE BANDS

All of the bands have been recorded in a short experimental campaign using the same experimental setup. Nevertheless the quality of the spectra depends on several factors: some bands are seriously overlapped, a few forbidden transitions are very weak, and the presence of strong atomic lines induces noise in some parts of the spectra.

We studied the bands one by one and when all the bands sharing the same upper electronic state were analyzed, they were gathered together and fitted simultaneously. Lines from bands linked to the two lowest states have been combined with microwave data (*13*), in order to increase the reliability of the derived parameters.

The energy level expression for the two low-lying $^2\Sigma^+$ states (251 cm^{-1} and 1574 cm^{-1}) was taken from Ref. (*19*). All the other spin–orbit components were fitted with the energy level expression

$$T = T_v + B_v J(J+1) - D_v J^2(J+1)^2 \pm \frac{1}{2}[p + p_J J(J+1)]\left(J + \frac{1}{2}\right). \qquad [1]$$

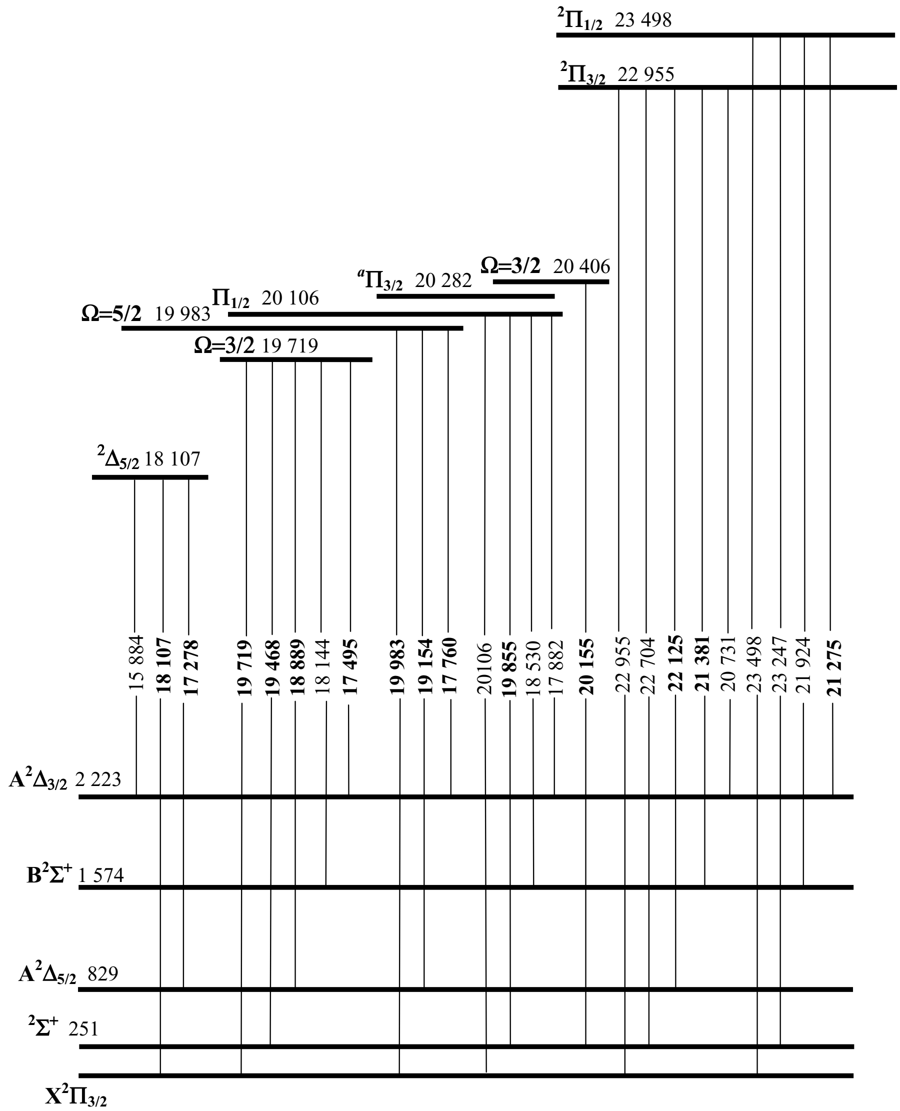

FIG. 1. Energy level diagram of NiF. Analyzed transitions are in boldface; the others are observed by laser-induced dispersed fluorescence. The state marked with a superscript "*a*" is from Ref. (*16*).

For one state (23 498 cm^{-1}) it has been necessary to introduce a phenomenological parameter $\pm a$ because the e and f levels have slightly different band origins. We note that Tanimoto *et al.* (*13*) did not use exactly the same polynomial expression to account for the rotational energy levels of the $X^2\Pi_{3/2}$ state, and this contributes to the differences between the two sets of parameters for the ground state.

We will now describe the studied bands. For the sake of clarity the states will be discussed in order of increasing energy of the upper electronic states as they appear in the energy level diagram (Fig. 1). We will consider hereafter that the nature of the 5 lower electronic components lying in the first 2500 cm^{-1} in the energy level diagram is firmly established from previous work, and comments are made only when a problem occurs. The energy level diagram (Fig. 1) includes all the observed transitions either analyzed in this paper or observed at low resolution by recording dispersed laser-induced fluorescence. All the experimental data for the studied bands ($\text{v}' = 0 - \text{v}'' = 0$) are collected in Table 1 and the derived parameters are summarized in Table 2.

1. The $[18.1]^2\Delta_{5/2}$ State

The $[18.1]^2\Delta_{5/2}$–$[0.83]A^2\Delta_{5/2}$ transition ($\nu_o = 17\,277.897$ cm^{-1}) is a very intense $\Delta\Omega = 0$ transition, and it is possible to follow the P and R branches up to $J = 82.5$. Splittings in the P and R branches are observed for $J \geq 60.5$. From a comparison with another transition (19 154 cm^{-1}), which involves the same $[0.83]A^2\Delta_{5/2}$ lower state, it can be shown that the splitting is mainly in the upper state. This splitting

TABLE 1
Observed Line Positions (in cm^{-1}) for All the ($v' = 0 - v'' = 0$) Studied Transitions of the ^{58}NiF Isotopomer

	$[18.1]^2\Delta_{5/2}$–$[0.83]A^2\Delta_{5/2}$		$[18.1]^2\Delta_{5/2}$–$X^2\Pi_{3/2}$					
J	R	P	Q_{ef}	Q_{fe}	R_{ee}	R_{ff}	P_{ee}	P_{ff}
2.5	17280.463							
3.5	17281.130	17275.084	18107.251	18107.251				
4.5	17281.829	17274.244	18107.148	18107.148	18111.331	18111.331		
5.5	17282.478	17273.387	18107.062	18107.062	18112.012	18112.012		
6.5	17283.118	17272.512	18106.959	18106.959	18112.624	18112.624		
7.5	17283.743	17271.609	18106.810	18106.810	18113.280	18113.280		
8.5	17284.336	17270.704	18106.669	18106.669	18113.899	18113.899		
9.5	17284.916	17269.756	18106.502	18106.502	18114.471	18114.471		
10.5	17285.478	17268.805	18106.353	18106.353	18115.062	18115.062		
11.5	17286.023	17267.830	18106.128	18106.128	18115.661	18115.602		
12.5	17286.542	17266.838	18105.906	18105.906	18116.188	18116.125		
13.5	17287.054	17265.830	18105.673			18116.656		18095.399
14.5	17287.539	17264.802	18105.392	18105.475	18117.229	18117.173	18094.501	18094.412
15.5	17288.005	17263.754	18105.117	18105.220		18117.643	18093.477	18093.377
16.5	17288.457	17262.687		18104.950		18118.097	18092.441	
17.5	17288.882	17261.604	18104.521	18104.645	18118.655	18118.533		18091.240
18.5	17289.300	17260.502	18104.199	18104.359	18119.122	18118.971	18090.338	18090.181
19.5	17289.700	17259.384	18103.861	18104.036	18119.559	18119.378	18089.289	18089.084
20.5	17290.061	17258.250	18103.487	18103.696	18119.959	18119.766	18088.166	18087.931
21.5	17290.410	17257.084	18103.086	18103.347		18120.121	18087.065	18086.814
22.5	17290.749	17255.913	18102.721	18102.984		18120.497	18085.935	18085.655
23.5	17291.069	17254.723	18102.276	18102.603	18121.160	18120.842		18084.465
24.5	17291.362	17253.517	18101.826	18102.228		18121.159	18083.659	18083.319
25.5	17291.648	17252.282	18101.378	18101.826	18121.865			18082.071
26.5	17291.909	17251.026	18100.923	18101.378	18122.210	18121.741	18081.318	18080.841
27.5	17292.157	17249.760	18100.428	18100.923	18122.507	18122.003	18080.130	18079.606
28.5	17292.379	17248.480	18099.918	18100.487		18122.210	18078.904	18078.350
29.5	17292.586	17247.182	18099.394	18100.006	18123.091	18122.507	18077.725	18077.050
30.5	17292.772	17245.863	18098.844	18099.546	18123.352	18122.651	18076.446	18075.777
31.5	17292.938	17244.526	18098.289	18099.032	18123.631	18122.858	18075.218	
32.5	17293.079	17243.171	18097.697	18098.540	18123.847	18123.023	18073.951	
33.5	17293.209	17241.802	18097.091	18098.010	18124.092	18123.173	18072.681	18071.753
34.5	17293.322	17240.408	18096.477	18097.467			18071.377	18070.377
35.5	17293.430	17239.002	18095.814	18096.936	18124.492		18070.102	18069.012
36.5		17237.578	18095.212	18096.362			18068.764	
37.5		17236.140	18094.500	18095.814	18124.872		18067.447	18066.187
38.5		17234.652	18093.834	18095.212	18125.051			18064.721
39.5		17233.196	18093.113	18094.630	18125.197		18064.789	18063.271
40.5		17231.695	18092.381	18093.987	18125.337		18063.411	18061.796
41.5		17230.153	18091.637	18093.377	18125.442		18062.024	18060.305
42.5		17228.632	18090.888	18092.745	18125.560		18060.636	
43.5		17227.083	18090.090	18092.095	18125.668		18059.282	18057.301
44.5		17225.520	18089.290	18091.433	18125.744			18055.725
45.5		17223.941	18088.479	18090.777			18056.447	18054.187
46.5		17222.341	18087.641	18090.090			18055.050	18052.594
47.5		17220.728	18086.815	18089.388				18051.003
48.5		17219.091	18085.934	18088.698				
49.5		17217.441	18085.036	18087.998				
50.5		17215.776	18084.126	18087.264				18046.108
51.5		17214.089	18083.217					18044.430
52.5		17212.390	18082.301	18085.795				
53.5		17210.672	18081.317	18085.036				
54.5		17208.938		18084.276				
55.5		17207.186						
56.5		17205.420		18082.742				
57.5		17203.629						
58.5		17201.837						

TABLE 1—*Continued*

J	$[18.1]^2\Delta_{5/2}$–$[0.83]A^2\Delta_{5/2}$ R_{ee}	R_{ff}	P_{ee}	P_{ff}
59.5			17200.023	17200.023
60.5			17198.198	17198.198
61.5			17196.333	17196.333
62.5	17289.057	17289.000	17194.462	17194.462
63.5	17288.646	17288.593	17192.580	17192.580
64.5	17288.222	17288.147	17190.697	17190.697
65.5	17287.774	17287.702	17188.799	17188.799
66.5	17287.315	17287.248	17186.883	17186.820
67.5	17286.828	17286.761	17184.959	17184.900
68.5	17286.337	17286.259	17183.000	17182.928
69.5	17285.822	17285.743	17181.022	17180.945
70.5	17285.302	17285.213	17179.025	17178.953
71.5	17284.751	17284.659	17177.038	17176.955
72.5	17284.220	17284.104	17175.025	17174.958
73.5	17283.638	17283.506	17172.976	17172.878
74.5	17283.024	17282.906	17170.931	18170.829
75.5	17282.415	17282.288	17168.873	18168.772
76.5	17281.768	17281.657	17166.795	18166.692
77.5	17281.129	17281.003	17164.707	18164.595
78.5	17280.461	17280.326	17162.608	18162.482
79.5	17279.778	17279.647	17160.501	18160.382
80.5	17279.076	17278.937	17158.346	18158.213
81.5	17278.392	17278.227	17156.196	18156.069
82.5			17154.075	18153.886
83.5			17151.875	18151.695

J	$[19.7]\Omega = 3/2$–$[0.25]^2\Sigma$ P_{ee}	Q_{fe}	R_{ff}	P_{ff}	Q_{ef}	R_{ee}	$[19.7]\Omega = 3/2$–$[0.83]^2\Delta_{5/2}$ Q
1.5						19470.723	
2.5						19472.316	
3.5		19470.428				19473.881	
4.5		19471.239	19466.714		19462.552	19475.412	
5.5		19471.993	19466.465		19461.558	19476.923	
6.5		19472.726	19466.238		19460.544	19478.412	18889.045
7.5		19473.459	19465.977		19459.55	19479.861	18888.916
8.5	19467.65	19474.116	19465.681	19452.03	19458.485	19481.307	18888.793
9.5	19467.599	19474.804	19465.385	19450.198	19457.408	19482.737	18888.585
10.5	19467.486	19475.438	19465.061	19448.356			18888.420
11.5	19467.355	19476.067	19464.71	19446.507	19455.215	19485.565	18888.198
12.5	19467.191	19476.687	19464.343	19444.619		19486.919	18887.965
13.5	19466.992	19477.258	19463.957	19442.742	19452.936	19488.282	18887.757
14.5	19466.816	19477.819	19463.546	19440.775	19451.779	19489.574	18887.486
15.5	19466.584	19478.358	19463.128	19438.853	19450.594	19490.875	18887.207
16.5	19466.369	19478.887	19462.667	19436.903	19449.393	19492.144	18886.919
17.5	19466.107	19479.376	19462.201	19434.907	19448.179	19493.4	18886.605
18.5	19465.827	19479.861	19461.732	19432.918	19446.943	19494.645	18886.260
19.5	19465.507	19480.327	19461.258	19430.888	19445.662	19495.834	18885.892
20.5	19465.18	19480.748	19460.714	19428.864	19444.381	19497.034	18885.543
21.5	19464.836		19460.15	19426.801	19443.066	19498.195	18885.181
22.5	19464.47	19481.554		19424.713	19441.75	19499.35	18884.763
23.5	19464.075	19481.921	19459.025	19422.625	19440.424	19500.449	18884.331
24.5	19463.661	19482.274	19458.392	19420.507	19439.057	19501.543	18883.923

TABLE 1—*Continued*

	$[19.7]\Omega = 3/2–[0.25]^2\Sigma$						$[19.7]\Omega = 3/2–[0.83]^2\Delta_{5/2}$
J	P_{ee}	Q_{fe}	R_{ff}	P_{ff}	Q_{ef}	R_{ee}	Q
25.5	19463.227	19482.600	19457.791	19418.376	19437.68	19502.631	18883.445
26.5	19462.769	19482.894	19457.151	19416.245	19436.296	19503.702	18882.947
27.5	19462.284	19483.166	19456.485	19414.070	19434.873	19504.711	18882.491
28.5	19461.807	19483.428	19455.827	19411.877	19433.416	19505.704	18881.939
29.5	19461.258	19483.659	19455.141	19409.658	19431.959	19506.685	18881.406
30.5	19460.714	19483.886	19454.410	19407.454	19430.491	19507.661	18880.882
31.5	19460.150	19484.076	19453.699	19405.205	19428.994	19508.597	18880.303
32.5	19459.550	19484.252	19452.936	19402.944	19427.464	19509.511	18879.731
33.5	19458.946	19484.415	19452.140	19400.677	19425.940	19510.42	18879.136
34.5	19458.311	19484.515	19451.383	19398.385	19424.391	19511.261	18878.488
35.5	19457.649		19450.542	19396.068	19422.830	19512.108	18877.876
36.5	19456.966		19449.727	19393.745	19421.244	19512.921	18877.211
37.5	19456.269		19448.865	19391.397	19419.633	19513.751	18876.548
38.5	19455.555		19448.015	19389.036	19418.004	19514.508	18875.848
39.5	19454.807		19447.153	19386.658	19416.375	19515.270	18875.161
40.5	19454.047		19446.240	19384.26	19414.714	19515.999	18874.421
41.5	19453.253		19445.328	19381.857	19413.029	19516.706	18873.660
42.5	19452.437		19444.381	19379.422	19411.338	19517.362	18872.900
43.5	19451.598		19443.451	19376.975	19409.622	19518.029	18872.151
44.5	19450.753		19442.482	19374.516	19407.894	19518.669	18871.323
45.5	19449.852		19441.512	19372.038	19406.141	19519.274	18870.514
46.5	19448.945		19440.492	19369.541	19404.381		18869.668
47.5	19448.015	19484.130		19367.032	19402.591	19520.429	18868.827
48.5	19447.068	19483.949	19438.421	19364.512	19400.801	19520.973	18867.962
49.5	19446.099	19483.759	19437.389	19361.967	19398.979	19521.461	18867.082
50.5	19445.101	19483.528	19436.296	19359.424	19397.152		
51.5	19444.080	19483.249			19395.299		18865.240
52.5	19443.066	19483.012			19393.435		18864.276
53.5	19441.983	19482.722			19391.552		18863.337
54.5	19440.883	19482.405					18862.386
55.5	19439.783						18861.356
56.5	19438.649						
57.5	19437.487						
58.5	19436.295						
59.5	19435.117						
60.5	19433.898						
61.5	19432.651						
62.5	19431.370						
63.5	19430.077						
64.5	19428.771						
65.5	19427.464						
66.5	19426.057						
67.5	19424.713						
68.5	19423.288						
69.5	19421.857						
70.5	19420.426						
71.5							
72.5	19417.428						
73.5	19415.904						
74.5	19414.361						
75.5	19412.794						
76.5	19411.208						

TABLE 1—*Continued*

	$[19.7]\Omega = 3/2–X^2\Pi_{3/2}$				$[19.7]\Omega = 3/2–[2.2]A^2\Delta_{3/2}$			
J	P_{ee}	P_{ff}	R_{ee}	R_{ff}	P_{ee}	P_{ff}	R_{ee}	R_{ff}
2.5	19717.012	19717.012	19721.564	19721.564				
3.5	19716.181	19716.181	19722.266	19722.266				
4.5	19715.358	19715.358	19722.966	19722.966				
5.5	19714.507	19714.507	19723.624	19723.624			17500.025	17500.025
6.5	19713.644	19713.644	19724.274	19724.274			17500.677	17500.677
7.5	19712.758	19712.758	19724.907	19724.907	17489.144	17489.144	17501.264	17501.264
8.5	19711.849	19711.849	19725.527	19725.527	17488.231	17488.231	17501.913	17501.913
9.5	19710.946	19710.946	19726.129	19726.129	17487.334	17487.334		
10.5	19710.016	19710.016	19726.726	19726.726	17486.351	17486.351	17503.057	17503.057
11.5	19709.065	19709.065	19727.283	19727.283	17485.423	17485.423	17503.656	17503.656
12.5	19708.100	19708.100	19727.826	19727.826	17484.420	17484.420	17504.163	17504.163
13.5	19707.106	19707.106	19728.363	19728.363	17483.419	17483.419	17504.651	17504.651
14.5	19706.144	19706.080	19728.928	19728.878	17482.396	17482.396	17505.164	17505.164
15.5	19705.163	19705.077	19729.444	19729.365	17481.390	17481.390	17505.667	17505.667
16.5	19704.149	19704.046	19729.943	19729.833	17480.326	17480.326	17506.160	17506.160
17.5	19703.119	19702.990	19730.423	19730.306	17479.280	17479.280	17506.586	17506.586
18.5	19702.069	19701.924	19730.895	19730.744	17478.200	17478.200	17507.028	17507.028
19.5	19701.016	19700.844	19731.339	19731.172	17477.110	17477.067	17507.403	17507.403
20.5	19699.931	19699.737	19731.769	19731.575	17475.999	17475.934	17507.854	17507.854
21.5	19698.846	19698.618	19732.194	19731.962	17474.868	17474.816	17508.218	17508.218
22.5	19697.770	19697.484	19732.606	19732.354	17473.662	17473.662	17508.556	17508.556
23.5	19696.615	19696.327	19733.017	19732.711	17472.553	17472.504	17508.872	17508.872
24.5	19695.476	19695.151	19733.370	19733.017	17471.366	17471.300	17509.198	17509.198
25.5	19694.334	19693.956		19733.370	17470.166	17470.092		
26.5	19693.170	19692.756	19734.087	19733.683	17468.921	17468.877		
27.5	19691.994	19691.523		19733.955	17467.719	17467.641	17510.082	17510.082
28.5	19690.806	19690.292	19734.719	19734.223	17466.443	17466.387	17510.325	17510.325
29.5	19689.600	19689.027	19735.043	19734.454	17465.177	17465.122	17510.541	17510.541
30.5	19688.383	19687.759	19735.309	19734.719	17463.884	17463.884	17510.815	17510.815
31.5	19687.158	19686.461	19735.595	19734.910	17462.561	17462.561	17511.032	17511.032
32.5	19685.917	19685.153	19735.867	19735.133	17461.208	17461.208	17511.195	17511.195
33.5	19684.661	19683.830	19736.100	19735.309	17459.895	17459.878	17511.347	17511.347
34.5	19683.401	19682.494	19736.349	19735.447	17458.523	17458.523	17511.478	17511.478
35.5	19682.117	19681.129	19736.578	19735.595	17457.157	17457.157	17511.625	17511.625
36.5	19680.826		19736.791	19735.726	17455.773	17455.773	17511.753	17511.753
37.5	19679.523	19678.364	19736.977	19735.867	17454.363	17454.363		
38.5	19678.204	19676.947	19737.151		17452.944	17452.944		
39.5	19676.889		19737.311		17451.502	17451.502		
40.5	19675.534	19674.088	19737.505		17450.047	17450.047		
41.5	19674.183	19672.624	19737.641		17448.573	17448.573		
42.5	19672.812	19671.132	19737.770		17447.086	17447.086		
43.5	19671.450	19669.652	19737.889		17445.583	17445.583		
44.5	19670.063	19668.144	19737.994		17444.061	17444.061		
45.5	19668.669	19666.619	19738.080		17442.525	17442.525		
46.5	19667.270	19665.083	19738.173		17440.970	17440.970		
47.5	19665.833		19738.238		17439.409	17439.409		
48.5	19664.418	19661.957	19738.295		17437.834	17437.847		
49.5	19662.980	19660.348			17436.206	17436.261		
50.5	19661.517	19658.756			17434.562	17434.641		
51.5	19660.074	19657.138			17432.930	17433.009		
52.5	19658.611	19655.510			17431.271	17431.375		
53.5	19657.138	19653.870			17429.612	17429.718		
54.5	19655.650	19652.182			17427.924	17428.059		
55.5	19654.128	19650.511			17426.228	17426.386		
56.5	19652.634	19648.836			17424.518	17424.689		
57.5	19651.111	19647.157			17422.795	17422.990		
58.5	19649.603	19645.424			17421.057	17421.270		
59.5	19648.063	19643.674			17419.300	17419.551		
60.5		19641.877			17417.527	17417.812		
61.5								
62.5	19643.419							

TABLE 1—*Continued*

	$[19.9]\Omega = 5/2$–$[0.83]A^2\Delta_{5/2}$				$[19.9]\Omega = 5/2$–$[0.83]A^2\Delta_{5/2}$		
J	P	R	Q	J	P	R	Q
2.5		19156.420		60.5	19075.497		
3.5	19151.046	19157.120		61.5	19073.696		
4.5	19150.215	19157.803	19153.618	62.5	19071.880		
5.5	19149.356	19158.456	19153.524	63.5	19070.052		
6.5	19148.483	19159.100	19153.402	64.5	19068.207		
7.5	19147.591	19159.728	19153.280	65.5	19066.349		
8.5	19146.676	19160.329	19153.137	66.5	19064.474		
9.5	19145.752	19160.920	19152.947	67.5	19062.584		
10.5	19144.798	19161.487	19152.754	68.5	19060.681		
11.5	19143.828	19162.040	19152.540	69.5	19058.761		
12.5	19142.854	19162.573	19152.339	70.5	19056.831		
13.5	19141.847	19163.086	19152.085	71.5	19054.892		
14.5	19140.820	19163.587	19151.843	72.5	19052.923		
15.5	19139.790	19164.066	19151.554	73.5	19050.950		
16.5	19138.741	19164.529	19151.262	74.5	19048.959		
17.5	19137.673	19164.968		75.5	19046.968		
18.5	19136.583	19165.397		76.5	19044.942		
19.5	19135.473	19165.799		77.5	19042.918		
20.5	19134.344	19166.184		78.5	19040.884		
21.5	19133.199	19166.547		79.5	19038.812		
22.5	19132.036	19166.900		80.5	19036.735		
23.5	19130.856	19167.237		81.5	19034.653		
24.5	19129.660	19167.551		82.5	19032.591		
25.5	19128.447	19167.843		83.5	19030.476		
26.5	19127.222	19168.146		84.5	19028.358		
27.5	19125.978	19168.394		85.5	19026.224		
28.5	19124.715	19168.647					
29.5	19123.436	19168.876					
30.5	19122.137	19169.092					
31.5	19120.822	19169.284					
32.5	19119.492	19169.455					
33.5	19118.143	19169.603					
34.5	19116.779	19169.742					
35.5	19115.397						
36.5	19114.001						
37.5	19112.591						
38.5							
39.5							
40.5							
41.5							
42.5	19105.215						
43.5	19103.704						
44.5	19102.176						
45.5	19100.634						
46.5	19099.071						
47.5	19097.494						
48.5	19095.898						
49.5	19094.287						
50.5	19092.657						
51.5	19091.007						
52.5	19089.345						
53.5	19087.661						
54.5	19085.979						
55.5	19084.270						
56.5	19082.544						
57.5	19080.803						
58.5	19079.051						
59.5	19077.280						

TABLE 1—*Continued*

	$[19.9]\Omega = 5/2–X^2\Pi_{3/2}$					
J	Q_{ef}	Q_{fe}	P_{ee}	P_{ff}	R_{ee}	R_{ff}
1.5					19985.1948	19985.195
2.5					19985.9118	19985.912
3.5					19986.6147	19986.615
4.5	19983.126	19983.126			19987.2957	19987.296
5.5	19983.043	19983.043			19987.9817	19987.982
6.5	19982.917	19982.917			19988.6167	19988.617
7.5	19982.811	19982.811			19989.2567	19989.257
8.5	19982.659	19982.659			19989.8767	19989.877
9.5	19982.501	19982.501			19990.4797	19990.480
10.5	19982.321	19982.321			19991.0617	19991.062
11.5	19982.146	19982.146			19991.6027	19991.603
12.5	19981.939	19981.939	19972.482	19972.411	19992.1707	19992.171
13.5	19981.678	19981.733	19971.495	19971.421	19992.7507	19992.679
14.5	19981.442	19981.504		19970.451	19993.2926	
15.5	19981.176	19981.261	19969.509		19993.7916	19993.664
16.5	19980.896	19981.005	19968.505	19968.371	19994.2846	19994.166
17.5	19980.597	19980.715		19967.306	19994.7586	19994.623
18.5	19980.271	19980.436	19966.396		19995.2306	19995.076
19.5	19979.946	19980.128	19965.359		19995.6856	19995.487
20.5		19979.813	19964.283	19964.062	19996.1156	19995.903
21.5	19979.226		19963.170	19962.926	19996.5286	19996.294
22.5	19978.848	19979.127	19962.068	19961.796	19996.9456	19996.660
23.5	19978.417	19978.766	19960.954	19960.625	19997.3516	19997.014
24.5	19978.008	19978.417	19959.814	19959.452	19997.6896	19997.352
25.5	19977.590	19978.008	19958.680	19958.258	19998.0696	19997.690
26.5	19977.150	19977.590	19957.518	19957.057	19998.4056	19997.958
27.5	19976.659	19977.150	19956.339	19955.828	19998.7806	19998.251
28.5	19976.179	19976.731	19955.148	19954.559	19999.0736	19998.507
29.5	19975.670	19976.292	19953.954	19953.327	19999.3926	19998.781
30.5	19975.146	19975.836	19952.732	19952.048	19999.7096	19999.012
31.5	19974.604	19975.360	19951.528		19999.9856	19999.207
32.5	19974.049	19974.877	19950.277	19949.441	20000.2125	19999.393
33.5	19973.468	19974.383	19949.024	19948.110	20000.4955	19999.575
34.5	19972.883	19973.867	19947.761	19946.763	20000.7365	19999.710
35.5	19972.268	19973.348	19946.490	19945.408	20000.9565	19999.872
36.5	19971.635	19972.827	19945.216	19944.008	20001.1715	19999.986
37.5	19970.989	19972.268	19943.926	19942.612	20001.3865	20000.110
38.5	19970.341	19971.703	19942.612	19941.250		20000.213
39.5	19969.656	19971.143	19941.250	19939.787	20001.7565	
40.5	19968.959	19970.563	19939.950	19938.335	20001.9215	
41.5	19968.236	19969.968	19938.617	19936.872	20002.0945	
42.5	19967.503	19969.372	19937.254	19935.387	20002.2285	
43.5	19966.771	19968.750	19935.881	19933.888	20002.3485	
44.5	19966.001	19968.130	19934.532	19932.386	20002.5065	
45.5	19965.220	19967.503	19933.135	19930.863	20002.5895	
46.5	19964.417	19966.843	19931.750		20002.7085	
47.5	19963.609	19966.195	19930.338	19927.745	20002.8005	
48.5	19962.766	19965.528	19928.935			
49.5	19961.930	19964.859	19927.523	19924.569		
50.5	19961.076	19964.172		19922.975		
51.5	19960.184	19963.468	19924.674	19921.351		
52.5	19959.290	19962.766	19923.216	19919.700		
53.5	19958.383	19962.068	19921.772	19918.044		
54.5	19957.453	19961.346	19920.301	19916.394		
55.5	19956.503	19960.625	19918.830	19914.704		
56.5	19955.541	19959.884	19917.358	19913.001		
57.5	19954.559	19959.140	19915.858	19911.280		
58.5	19953.576	19958.383	19914.376	19909.565		

TABLE 1—*Continued*

J	Q_{ef}	Q_{fe}	P_{ee}	P_{ff}	R_{ee}	R_{ff}
	[19.9]$\Omega = 5/2$–$X^2\Pi_{3/2}$					
59.5	19952.565	19957.624	19912.860	19907.799		
60.5	19951.528	19956.859	19911.381	19906.042		
61.5	19950.503	19956.080	19909.866	19904.271		
62.5	19949.441	19955.313	19908.369	19902.475		
63.5	19948.374	19954.559		19900.680		
64.5	19947.292	19953.719		19898.847		
65.5	19946.201	19952.932		19897.000		
66.5	19945.069	19952.130				
67.5	19943.926	19951.328				
68.5	19942.808	19950.503				
69.5	19941.637	19949.677				
70.5	19940.470	19948.859				
71.5	19939.292	19948.026				
72.5	19938.076	19947.199				
73.5	19936.864	19946.366				
74.5	19935.633	19945.511				
75.5	19934.374					
76.5	19933.135	19943.832				
77.5	19931.841	19942.966				
78.5	19930.571	19942.103				
79.5	19929.289	19941.249				
80.5	19927.983	19940.376				
81.5	19926.651	19939.527				

J	Q_{ef}	Q_{fe}	P_{ee}	P_{ff}	R_{ee}	R_{ff}
	[19.9]$\Omega = 5/2$–[2.2]$A^2\Delta_{3/2}$					
1.5					17761.591	17761.591
2.5	17759.667	17759.667			17762.322	17762.322
3.5	17759.619	17759.619			17763.022	17763.022
4.5	17759.527	17759.527			17763.711	17763.711
5.5	17759.435	17759.435			17764.366	17764.366
6.5	17759.320	17759.320			17765.010	17765.010
7.5	17759.183	17759.183			17765.655	17765.655
8.5	17759.021	17759.021			17766.261	17766.261
9.5	17758.858	17758.858			17766.833	17766.833
10.5	17758.673	17758.673			17767.398	17767.398
11.5	17758.461	17758.504			17767.939	17767.939
12.5	17758.233	17758.298			17768.522	17768.477
13.5	17757.997	17758.036			17769.038	17768.990
14.5	17757.732	17757.799			17769.536	17769.489
15.5	17757.464	17757.524			17770.037	17769.965
16.5	17757.160	17757.223			17770.505	17770.435
17.5	17756.855	17756.938	17743.638	17743.591	17770.942	17770.875
18.5	17756.525	17756.596	17742.569	17742.500	17771.380	17771.307
19.5	17756.185	17756.253	17741.466		17771.786	17771.715
20.5	17755.809	17755.887	17740.339	17740.269	17772.188	17772.106
21.5	17755.435	17755.517		17739.135	17772.562	17772.486
22.5	17755.036	17755.118	17738.063	17737.999	17772.925	17772.847
23.5	17754.620	17754.700	17736.906	17736.804	17773.278	17773.183
24.5	17754.187	17754.279	17735.711	17735.611	17773.589	17773.512
25.5	17753.734	17753.829	17734.495	17734.406	17773.899	17773.810
26.5	17753.264	17753.365	17733.301	17733.187	17774.191	17774.103
27.5	17752.772	17752.876	17732.051	17731.941	17774.462	17774.361
28.5	17752.270	17752.386	17730.803	17730.684	17774.724	17774.638
29.5	17751.749	17751.865			17774.959	17774.853
30.5	17751.216	17751.336			17775.194	17775.067
31.5	17750.664	17750.787			17775.419	17775.263

TABLE 1—*Continued*

J	Q_{ef}	Q_{fe}	P_{ee}	P_{ff}	R_{ee}	R_{ff}
	$[19.9]\Omega = 5/2$–$[2.2]A^2\Delta_{3/2}$					
32.5	17750.086	17750.219			17775.608	17775.474
33.5	17749.502	17749.638			17775.763	17775.608
34.5	17748.906	17749.034			17775.895	17775.763
35.5	17748.265	17748.414				
36.5	17747.632	17747.779				
37.5	17746.982	17747.127				
38.5	17746.301	17746.458				
39.5	17745.611	17745.776				
40.5	17744.916	17745.081				
41.5	17744.194	17744.362				
42.5	17743.451	17743.638				
43.5	17742.696	17742.890				
44.5	17741.925	17742.125				
45.5	17741.139	17741.343				
46.5	17740.339	17740.546				
47.5	17739.515	17739.730				
48.5	17738.678	17738.907				
49.5	17737.822	17738.063				
50.5	17736.955	17737.208				
51.5	17736.066	17736.330				
52.5	17735.163	17735.420				
53.5	17734.247	17734.530				
54.5	17733.306	17733.637				
55.5	17732.373	17732.707				
56.5	17731.394	17731.766				
57.5	17730.432	17730.803				

J	Q_{fe}	Q_{ef}	P_{ee}	R_{ff}
	$[20.1]^2\Pi_{1/2}$–$[0.25]^2\Sigma$			
1.5	19856.284			
2.5	19857.168			
3.5	19858.069			
4.5	19858.934			
5.5	19859.774			
6.5	19860.647			
7.5	19861.481	19846.811		
8.5	19862.318	19845.801		
9.5	19863.122	19844.797		
10.5	19863.927	19843.769		
11.5	19864.725	19842.732		
12.5	19865.499	19841.687	19854.709	
13.5	19866.287	19840.650	19854.612	19853.186
14.5	19867.045	19839.590	19854.510	19852.986
15.5	19867.791	19838.522	19854.394	19852.775
16.5	19868.530	19837.439	19854.287	19852.566
17.5	19869.259	19836.351		19852.330
18.5	19869.973	19835.255		19852.119
19.5	19870.676	19834.190		19851.850
20.5	19871.370	19833.057	19853.701	
21.5	19872.049	19831.938	19853.529	19851.331
22.5	19872.726	19830.809	19853.337	19851.072
23.5	19873.373	19829.657	19853.132	19850.777
24.5	19874.028	19828.530	19852.920	19850.497
25.5	19874.659	19827.382	19852.701	19850.193
26.5	19875.282	19826.216	19852.470	19849.899
27.5	19875.888	19825.055	19852.234	19849.565
28.5	19876.491	19823.868	19851.981	19849.227
29.5	19877.083	19822.683		19848.878
30.5	19877.650	19821.495	19851.451	19848.516
31.5	19878.222	19820.298	19851.161	19848.198
32.5	19878.772	19819.096	19850.868	19847.814
33.5	19879.312	19817.884	19850.546	19847.457
34.5	19879.839	19816.665	19850.251	19847.081
35.5	19880.356	19815.434	19849.899	19846.696
36.5	19880.848	19814.204	19849.565	19846.302
37.5	19881.340	19812.967	19849.227	19845.907
38.5	19881.819	19811.714	19848.878	19845.492
39.5	19882.275	19810.485	19848.516	19845.078
40.5	19882.740	19809.205	19848.137	19844.678
41.5	19883.184	19807.938	19847.744	19844.229
42.5	19883.609	19806.668	19847.339	19843.769
43.5	19884.022	19805.396	19846.930	19843.329
44.5	19884.426		19846.505	19842.872
45.5	19884.838	19802.819	19846.083	19842.410
46.5	19885.207	19801.529	19845.633	19841.945

TABLE 1—*Continued*

	$[20.1]^2\Pi_{1/2}$–$[0.25]^2\Sigma$			
J	Q_{fe}	Q_{ef}	P_{ee}	R_{ff}
47.5	19885.584	19800.230	19845.174	19841.470
48.5	19885.937	19798.919	19844.678	19840.974
49.5	19886.271	19797.610	19844.229	19840.484
50.5	19886.628	19796.293	19843.759	19840.023
51.5	19886.925	19794.987	19843.246	19839.477
52.5	19887.239	19793.674	19842.732	19838.986
53.5	19887.533	19792.343	19842.220	19838.462
54.5	19887.815	19791.010	19841.687	19837.934
55.5	19888.079	19789.688	19841.150	19837.439
56.5	19888.329	19788.343	19840.604	19836.871
57.5	19888.575	19787.013	19840.021	19836.347
58.5	19888.785	19785.640	19839.475	19835.801
59.5	19889.016	19784.302	19838.880	19835.257
60.5	19889.218	19782.911		19834.684
61.5	19889.401	19781.603	19837.686	19834.128
62.5			19837.062	19833.544
63.5	19889.782		19836.447	19832.963
64.5	19889.917		19835.804	19832.384

	$[20.1]^2\Pi_{1/2}$–$[0.25]^2\Sigma$			
J	Q_{fe}	Q_{ef}	P_{ee}	R_{ff}
65.5	19890.087		19835.159	
66.5	19890.218		19834.516	19831.223
67.5	19890.329		19833.851	19830.635
68.5	19890.425		19833.158	19830.026
69.5	19890.524		19832.487	19829.418
70.5				19828.826
71.5			19831.085	19828.172
72.5			19830.392	19827.600
73.5			19829.657	19826.970
74.5			19828.904	19826.355
75.5			19828.172	
76.5			19827.382	
77.5			19826.651	
78.5			19825.869	
79.5			19825.055	
80.5			19824.281	
81.5			19823.490	
82.5			19822.683	

	$[20.4]\Pi_{1/2}$–$[0.25]^2\Sigma$	
J	Q_{ef}	Q_{fe}
4.5	20149.254	
5.5	20148.271	
6.5	20147.242	
7.5	20146.212	
8.5	20145.153	
9.5	20144.099	20161.454
10.5	20142.970	20162.078
11.5	20141.820	20162.681
12.5	20140.694	20163.271
13.5	20139.525	20163.832
14.5	20138.344	20164.345
15.5	20137.114	20164.863
16.5	20135.887	20165.416
17.5		20165.834
18.5	20133.345	20166.273
19.5	20132.062	20166.705
20.5	20130.735	20167.094
21.5	20129.398	20167.456
22.5	20128.037	20167.818
23.5	20126.649	20168.168
24.5	20125.263	20168.448
25.5	20123.819	20168.773
26.5	20122.393	20169.027
27.5	20120.943	20169.255
28.5	20119.447	20169.465
29.5	20117.954	20169.657
30.5	20116.451	20169.821
31.5	20114.899	20169.976

	$[20.4]\Pi_{1/2}$–$[0.25]^2\Sigma$	
J	Q_{ef}	Q_{fe}
32.5	20113.349	20170.101
33.5	20111.777	20170.199
34.5	20110.252	
35.5	20108.598	
36.5	20106.968	
37.5	20105.320	
38.5	20103.661	
39.5	20101.982	
40.5	20100.285	
41.5	20098.574	
42.5	20096.848	
43.5	20095.112	
44.5	20093.351	
45.5	20091.581	
46.5	20089.801	
47.5		
48.5	20086.172	
49.5	20084.346	
50.5	20082.511	
51.5	20080.661	
52.5	20078.790	
53.5	20076.908	
54.5	20075.021	
55.5	20073.119	
56.5	20071.211	
57.5	20069.292	
58.5	20067.368	

TABLE 1—*Continued*

J	$[22.9]^2\Pi_{3/2}$–$[1.5]B^2\Sigma^+$					
	Q_{ef}	Q_{fe}	P_{ee}	P_{ff}	R_{ee}	R_{ff}
1.5		21381.833				
2.5		21382.277				
3.5						
4.5		21383.046	21379.627		21387.216	
5.5	21377.942	21383.427	21379.277		21388.380	
6.5	21377.382	21383.828	21378.861		21389.501	
7.5	21376.833	21384.168	21378.492		21390.617	
8.5	21376.252		21378.060		21391.696	
9.5	21375.626	21384.839	21377.642	21368.433	21392.807	
10.5	21375.036	21385.139	21377.183	21367.034	21393.903	
11.5	21374.436		21376.767	21365.676	21394.951	
12.5	21373.780	21385.755	21376.253	21364.287	21395.979	
13.5	21373.167	21386.036	21375.786	21362.927	21397.023	
14.5	21372.484	21386.293	21375.259	21361.495	21398.044	
15.5	21371.812	21386.553	21374.790		21399.034	
16.5	21371.128	21386.776	21374.257	21358.636	21400.018	
17.5	21370.428	21387.004	21373.696	21357.151	21401.008	
18.5	21369.728	21387.216	21373.165	21355.704	21401.979	
19.5	21368.997	21387.403	21372.620	21354.229	21402.937	
20.5	21368.284	21387.596	21372.039	21352.698	21403.856	
21.5	21367.516	21387.749	21371.462	21351.248	21404.782	
22.5	21366.743	21387.893	21370.851	21349.687	21405.694	
23.5	21365.964	21388.039	21370.237	21348.152	21406.555	
24.5	21365.166	21388.165	21369.584	21346.623	21407.465	
25.5	21364.369	21388.279	21368.957	21345.055	21408.333	
26.5	21363.556	21388.379	21368.284	21343.473	21409.170	
27.5	21362.709	21388.456		21341.898	21410.010	
28.5	21361.871	21388.529	21366.941	21340.291	21410.837	
29.5	21361.008		21366.235	21338.701	21411.633	21384.093
30.5	21360.140		21365.507	21337.071	21412.449	21383.966
31.5	21359.258		21364.835	21335.434	21413.198	21383.829
32.5	21358.352		21364.084		21413.981	21383.702
33.5	21357.441		21363.346	21332.136	21414.717	21383.533
34.5	21356.519		21362.556	21330.448	21415.493	21383.345
35.5	21355.584		21361.809	21328.764	21416.198	21383.197
36.5	21354.624		21361.007	21327.073	21416.894	21382.982
37.5	21353.663			21325.361		21382.761
38.5	21352.696		21359.371	21323.647	21418.275	21382.525
39.5	21351.702		21358.577	21321.868	21418.963	21382.279
40.5	21350.699		21357.690	21320.123	21419.599	21382.020
41.5	21349.689		21356.882	21318.345	21420.229	21381.783
42.5	21348.660		21355.964	21316.591	21420.859	21381.497
43.5	21347.593		21355.076	21314.801	21421.470	21381.185
44.5	21346.559		21354.226	21313.001	21422.079	21380.891
45.5	21345.488		21353.308	21311.198	21422.655	21380.566
46.5	21344.415		21352.370	21309.353	21423.195	21380.226
47.5	21343.315			21307.541	21423.759	21379.892
48.5	21342.211			21305.681	21424.297	21379.524
49.5	21341.105			21303.839	21424.802	21379.132
50.5	21339.974			21301.973	21425.309	21378.729
51.5	21338.831				21425.821	21378.360
52.5	21337.683				21426.316	21377.943
53.5	21336.514				21426.730	21377.471
54.5	21335.323				21427.185	
55.5	21334.139				21427.616	
56.5	21332.919					
57.5	21331.665					
58.5	21330.448					

TABLE 1—*Continued*

J	$[22.9]^2\Pi_{3/2}$–$[0.83]^2\Delta_{5/2}$ Q	P	R	J	$[22.9]^2\Pi_{3/2}$–$[0.83]^2\Delta_{5/2}$ Q	P	R
3.5	22125.584			32.5	22115.543	22090.963	
4.5	22125.482			33.5	22114.921	22089.590	22140.292
5.5	22125.380			34.5	22114.287	22088.196	22140.090
6.5	22125.267		22130.939	35.5	22113.622	22086.779	22139.847
7.5	22125.112		22131.547	36.5	22112.937	22085.357	22139.610
8.5	22124.984	22118.525	22132.144	37.5	22112.251	22083.921	22139.366
9.5	22124.769	22117.598		38.5	22111.569	22082.436	22139.052
10.5	22124.594	22116.628	22133.304	39.5	22110.806	22080.954	22138.711
11.5	22124.368	22115.663	22133.885	40.5	22110.042	22079.469	22138.421
12.5	22124.129	22114.667	22134.362	41.5	22109.250	22077.908	22138.077
13.5	22123.869	22113.622	22134.884	42.5	22108.501	22076.392	22137.757
14.5	22123.608	22112.628	22135.382	43.5	22107.657	22074.838	22137.383
15.5	22123.324	22111.569	22135.819	44.5	22106.845	22073.267	22136.975
16.5	22123.011	22110.520	22136.257	45.5	22106.001	22071.679	22136.577
17.5	22122.688	22109.428	22136.698	46.5	22105.137	22070.075	22136.139
18.5	22122.336	22108.320	22137.101	47.5	22104.262	22068.459	22135.687
19.5	22121.970	22107.190	22137.488	48.5	22103.372	22066.822	22135.240
20.5	22121.582	22106.040	22137.853	49.5	22102.448	22065.161	22134.755
21.5	22121.192	22104.907	22138.231	50.5	22101.511	22063.489	22134.277
22.5	22120.768	22103.717	22138.560	51.5	22100.580	22061.804	22133.711
23.5	22120.330	22102.525	22138.876	52.5	22099.617	22060.102	
24.5	22119.870	22101.319	22139.170	53.5	22098.635	22058.372	
25.5	22119.408	22100.084	22139.452	54.5	22097.611	22056.635	
26.5	22118.910	22098.851	22139.719	55.5	22096.605	22054.872	
27.5	22118.379	22097.611	22139.969	56.5	22095.545	22053.087	
28.5	22117.854	22096.279	22140.202	57.5	22094.449	22051.284	
29.5	22117.305	22094.984	22140.377	58.5	22093.409		
30.5	22116.733	22093.656	22140.566	59.5	22092.313		
31.5	22116.155	22092.313	22140.715	60.5	22091.212		

J	$[23.5]^2\Pi_{1/2}$–$[2.2]A^2\Delta_{3/2}$ Q_{ef}	Q_{fe}	P_{ee}	P_{ff}	R_{ee}	R_{ff}
1.5	21274.546					
2.5	21274.456				21277.128	
3.5	21274.278				21277.754	21278.455
4.5	21274.144				21278.347	21279.170
5.5	21273.943				21278.918	21279.935
6.5	21273.759		21268.993		21279.484	21280.652
7.5	21273.546		21268.046		21280.055	21281.343
8.5	21273.323		21267.102		21280.598	21281.970
9.5	21273.083		21266.055	21267.352	21281.120	21282.654
10.5	21272.805		21265.078	21266.488	21281.586	21283.273
11.5	21272.520			21265.553	21282.065	21283.916
12.5	21272.246		21262.966	21264.700	21282.554	21284.501
13.5	21271.904		21261.914		21282.989	21285.073
14.5	21271.570		21260.785	21262.788	21283.397	21285.701
15.5	21271.211			21261.791	21283.799	21286.244
16.5	21270.862		21258.566		21284.213	21286.730
17.5	21270.477		21257.449	21259.834	21284.607	21287.237
18.5	21270.054		21256.278	21258.804	21284.953	21287.756
19.5	21269.640	21272.724	21255.111	21257.762	21285.270	
20.5	21269.194		21253.897	21256.678	21285.569	21288.695
21.5	21268.732	21272.110	21252.717	21255.666	21285.880	21289.105
22.5	21268.263	21271.791	21251.472	21254.549	21286.184	21289.549

TABLE 1—*Continued*

	$[23.5]^2\Pi_{1/2}$–$[2.2]A^2\Delta_{3/2}$					
J	Q_{ef}	Q_{fe}	P_{ee}	P_{ff}	R_{ee}	R_{ff}
23.5	21267.769	21271.431	21250.220		21286.457	
24.5	21267.234	21271.089	21248.954	21252.321	21286.691	21290.319
25.5	21266.721	21270.715	21247.655	21251.184	21286.921	21290.704
26.5	21266.171	21270.315	21246.378	21249.999		21291.040
27.5	21265.609	21269.892	21245.076	21248.842	21287.328	21291.371
28.5	21265.027	21269.485	21243.754	21247.656	21287.504	21291.696
29.5		21268.993	21242.399			21291.990
30.5		21268.527	21240.973	21245.203		21292.261
31.5	21263.160	21268.045	21239.643	21243.968		21292.536
32.5	21262.502	21267.565	21238.247	21242.728		21292.779
33.5	21261.860	21267.039	21236.830	21241.456		21293.024
34.5	21261.159	21266.488	21235.397	21240.152		21293.221
35.5	21260.437	21265.922	21233.942	21238.866		21293.420
36.5	21259.734	21265.373	21232.488	21237.493		21293.615
37.5	21259.007	21264.777	21231.014	21236.159		21293.743
38.5	21258.219	21264.176	21229.491	21234.828		21293.865
39.5	21257.449	21263.582	21227.997	21233.425		21293.997
40.5	21256.678	21262.915		21232.031		21294.096
41.5	21255.861	21262.254		21230.604		21294.180
42.5	21255.049	21261.595				21294.251
43.5	21254.187	21260.910				
44.5						
45.5	21252.472	21259.443				
46.5	21251.580	21258.711				
47.5	21250.667	21257.936				
48.5	21249.763	21257.157				
49.5	21248.842	21256.385				
50.5	21247.859	21255.546				
51.5	21246.884					
52.5	21245.898					

TABLE 2
Molecular Constants (in cm^{-1}) of the v = 0 Vibronic States of NiF (All Uncertainties Are 1 σ)

	T_0	B_0	$D_0 \times 10^7$	a	p	$p_J \times 10^5$	γ	$\gamma_D \times 10^5$
$^2\Pi_{1/2}$	23 498.3710(36)	.3794255(81)	5.116(34)	−.0791(39)	−.14843(30)	.157(20)		
$^2\Pi_{3/2}$	22 955.1953(20)	.3791837(22)	5.150(10)					
$\Omega = 3/2$[c]	20 405.7131(33)	.3786401(35)	3.843(30)					
$^2\Pi_{1/2}$[a]	*20 281.96(7)*	*.3844(1)*	*6.5(5)*			*−1.2(4)*		
$\Pi_{1/2}$	20 106.2940(19)	.3848634(32)	5.070(60)		−.09487(10)	.4066(38)		
$\Omega = 5/2$	19 983.3271(15)	.3795417(13)	4.902(22)					
$\Omega = 3/2$	19 718.9750(15)	.3796006(26)	5.182(30)			−.2634(28)		
$^2\Delta_{5/2}$	18 107.3732(12)	.3791866(18)	4.988(10)			.025(2)		
$A^2\Delta_{3/2}$	2 223.5743(15)	.3884270(32)	5.551(24)		−.00288(10)	−.0890(54)		
$B^2\Sigma^+$	1 574.1057(20)	.3860004(43)	5.248(14)				−.14947(14)	.1055(76)
$A^2\Delta_{5/2}$	829.4761(14)	.3885599(23)	5.427(10)					
$^2\Sigma$	251.2522(14)	.3900119(15)	5.494(29)				−.959965(58)	1.82254(43)
		.390016166(37)[b]	*5.58023(93)*[b]				*−.9597221(18)*[b]	*1.79087(32)*[b]
$X^2\Pi_{3/2}$	0	.3878134(12)	6.088(24)			−2.3160(36)		
		.387816528(28)[b]	*6.15136(67)*[b]			*−2.31740(33)*[b]		

[a] From Ref. (*16*).
[b] From Ref. (*13*).
[c] From Ref. (*10*). $H = 0.135(10) \times 10^{-10} cm^{-1}$ and $L = -0.521(30) \times 10^{-15} cm^{-1}$.

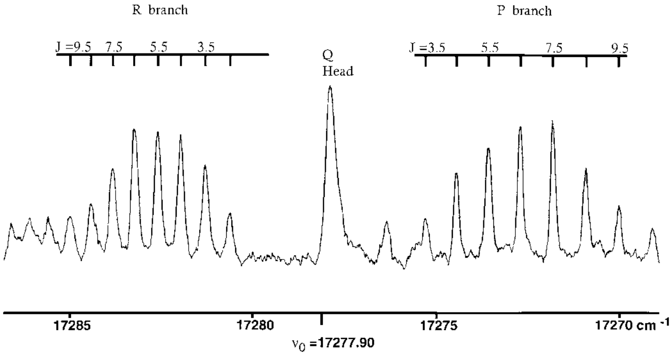

FIG. 2. Laser-induced dispersed fluorescence of the first lines of the $[18.1]^2\Delta_{5/2}$–$[0.83]A^2\Delta_{5/2}$ transition ($\nu_o = 17\,277.897$ cm^{-1}) of NiF. The broadband laser line (1 cm^{-1}) is located on the Q head of the $[18.1]^2\Delta_{5/2}$–$X^2\Pi_{3/2}$ transition (18 107.373 cm^{-1}).

is proportional to J^3 and is rarely observed in $\Omega = 5/2$ spin–orbit components. Nevertheless, there is no doubt that the two states linked by this transition are $\Omega = 5/2$ spin–orbit components for two reasons. First, a dispersed laser-induced fluorescence experiment shows clearly that the first R line has $J'' = 2.5$ (Fig. 2). Second, the upper state is linked to the ground $X^2\Pi_{3/2}$ state by a transition in which Q branches are observed. This second transition $[18.1]^2\Delta_{5/2}$–$X^2\Pi_{3/2}$ ($\nu_o =$ 18107.373 cm^{-1}) is also intense but blended with several other transitions, and lines from the six expected branches have been identified up to $J = 56.5$. As already noted, the experimental microwave data determined by Tanimoto *et al.* (*13*) have been included in the fitting procedure. In the emission spectrum, a very weak R head is observed at 15 900 cm^{-1} which could be attributed to the forbidden $[18.1]^2\Delta_{5/2}$–$[2.2]A^2\Delta_{3/2}$ (15 883.800 cm^{-1}) transition, but no signal is observed either in emission or in dispersed fluorescence experiments which could be associated with a transition between the upper $[18.1]^2\Delta_{5/2}$ state and either of the lower $^2\Sigma$ states.

2. The $[19.7]\Omega = 3/2$ State

This state is linked to all of the 5 lower electronic components by more or less intense transitions, which can be rotationally analyzed. Four transitions have been fitted simultaneously: $[19.7]\Omega = 3/2$–$X^2\Pi_{3/2}$ ($\nu_o = 19\,718.975$ cm^{-1}) (Fig. 3), $[19.7]\Omega = 3/2$–$[0.25]^2\Sigma^+$ ($\nu_o = 19\,467.723$ cm^{-1}), $[19.7]\,\Omega =$ $3/2$–$[0.83]A^2\Delta_{5/2}$ ($\nu_o = 18\,889.499$ cm^{-1}), and $[19.7]\ \Omega =$ $3/2$–$[2.2]A^2\Delta_{3/2}$ ($\nu_o = 17\,495.401$ cm^{-1}). The fifth transition $[19.7]\Omega = 3/2$–$[1.5]B^2\Sigma^+$($\nu_o = 18\,144.869$ cm^{-1}) has been studied in a previous paper (*8*) by dispersed laser-induced fluorescence. This band happens to be completely overlapped by the intense $[18.1]^2\Delta_{5/2}$–$X^2\Pi_{3/2}$ ($\nu_o = 18\,107.373$ cm^{-1}) transition, and thus we cannot pick out enough lines to characterize the lower $[1.5]B^2\Sigma^+$ state. The presence or absence of Q branches in the transitions involving a lower $^2\Delta$ or $^2\Pi$ spin–orbit component indicates that the upper state must be a $\Omega = 3/2$ state. However, the relative intensities of the bands do not allow us to attribute a symmetry to the upper state. If we assume that the $[19.7]\Omega = 3/2$ state is a $^2\Delta_{3/2}$ state, it agrees with the relative intensities of the weak $[19.7]\Omega = 3/2$–$[0.83]A^2\Delta_{5/2}$ ($\nu_o =$ 18 889.499 cm^{-1}) and the intense $[19.7]\Omega = 3/2$–$[2.2]A^2\Delta_{3/2}$ ($\nu_o = 17\,495.401$ cm^{-1}) transitions. However, this hypothesis is inconsistent with intense transitions connecting to $^2\Sigma^+$ states. On the other hand, an upper $^2\Pi_{3/2}$ spin–orbit component agrees with the presence of transitions to $^2\Sigma^+$ states, but it does not conform to the usual selection rules when we consider transitions to the spin–orbit components of the $A^2\Delta$ state and that the

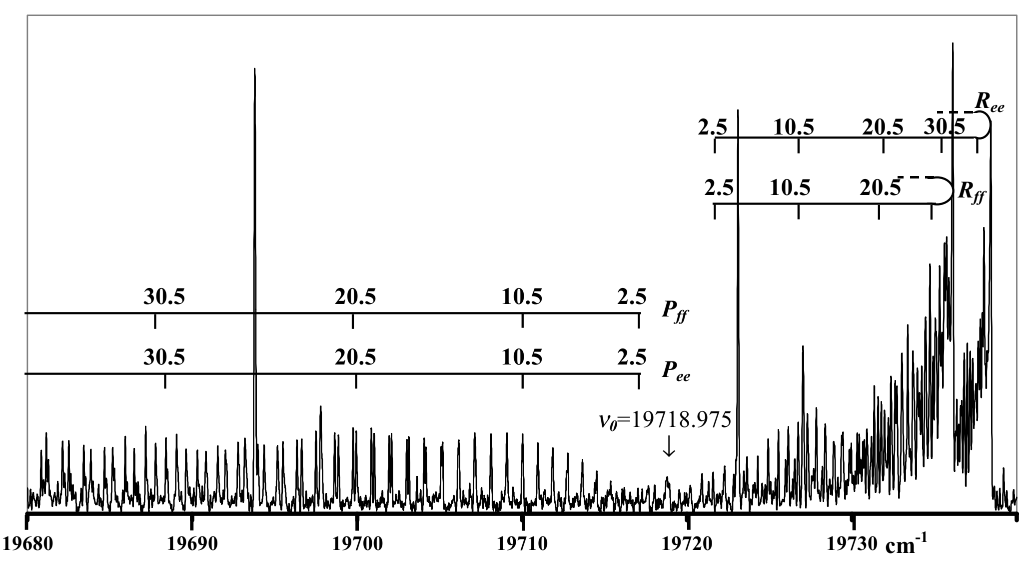

FIG. 3. The $[19.7]\Omega = 3/2$–$X^2\Pi_{3/2}$ 0–0 transition of NiF.

$[19.7]\Omega = 3/2$–$[2.2]A^2\Delta_{3/2}$ ($\nu_o = 17\,495.401$ cm^{-1}) transition is one of the three most intense transitions. We note that the same situation occurs in the spectrum of NiCl: a $[21.6]\Omega = 3/2$ state located at 21 608 cm^{-1} in the energy level diagram (*20*) is linked to all five low-lying electronic states. About 720 spectral lines have been fitted simultaneously. The presence in the data file of the microwave data for the two lowest states breaks the correlation between the contributions to the fine structure of the upper state and the $X^2\Pi_{3/2}$ state. This enables a reliable determination of the p_J parameter of the upper state. Curiously, it has been necessary to introduce a small lambda-doubling ($p = -0.00288$ cm^{-1}) parameter in the lower $[2.2]A^2\Delta_{3/2}$ state to account for the e/f splitting. The relative positions of four of the lower states, $X^2\Pi_{3/2}$, $[0.25]^2\Sigma^+$, $[0.83]A^2\Delta_{5/2}$, and $[2.2]A^2\Delta_{3/2}$, are now very well determined.

3. The $[19.9]\Omega = 5/2$ State

This state is linked to the lower electronic components by two intense transitions: the $[19.9]\Omega = 5/2$–$X^2\Pi_{3/2}$ ($\nu_o = 19\,983.327$ cm^{-1}) and the $[19.9]\Omega = 5/2$–$[0.83]A^2\Delta_{5/2}$ ($\nu_o = 19\,153.851$ cm^{-1}) transitions. A weak transition, $[19.9]\Omega = 5/2-[2.2]A^2\Delta_{3/2}$ ($\nu_o = 17\,759.753$ cm^{-1}), has been already studied in a previous paper (*7*) on the basis of a laser excitation spectrum, the quality of which is equivalent to the emission spectra recorded by Fourier transform spectroscopy. As a consequence it was possible to include lines collected by the two experimental techniques in a simultaneous fit. As usual the microwave data (*13*) of the ground state have been added to the fit that includes 670 rotational lines. The $[19.9]\Omega = 5/2$–$[0.83]A^2\Delta_{5/2}$ ($\nu_o = 19\,153.851$ cm^{-1}) transition is the most intense band observed in the emission spectrum. In this transition, it has been possible to observe rotational lines in the P branch up to $J = 85.5$ without any doubling. This absence is consistent with the assumption that the splitting observed in the lines of the $[18.1]^2\Delta_{5/2}$–$[0.83]A^2\Delta_{5/2}$ ($\nu_o = 17\,277.897$ cm^{-1}) transition arises mainly from a lambda doubling in the upper state. Both the selection rules and the relative intensities of the three bands suggest that the upper state has $\Omega = 5/2$. The hypothesis of a $^2\Delta_{5/2}$ state is consistent with the fact that as for NiCl (*19*) there is a $^2\Delta_{5/2}$ (21 905 cm^{-1}) state that is linked to the lower $X^2\Pi_{3/2}$, $A^2\Delta_{5/2}$, and $A^2\Delta_{3/2}$ states. However, an additional $^2\Delta_{5/2}$ state has been already identified at 18 100 cm^{-1}, while theoretical calculations (*12*) do not suggest the presence of two $^2\Delta_i$ electronic states in the 17 000 cm^{-1}–22 000 cm^{-1} spectral range. The necessity of a small lambda-doubling ($p = -0.00288$ cm^{-1}) parameter in the lower $[2.2]A^2\Delta_{3/2}$ state to account for the e/f splitting is also confirmed. We can note that 12 Q lines have been observed in the $[19.9]\Omega = 5/2$–$[0.83]A^2\Delta_{5/2}$ ($\nu_o = 19\,153.851$ cm^{-1}) transition and their rapidly decreasing intensity is consistent with a $\Delta\Omega = 0$ transition.

4. The [20.1] $\Pi_{1/2}$ State

Dispersed laser-induced fluorescence showed that this upper state is linked to all the low-lying states except the $[0.83]A^2\Delta_{5/2}$ state. The $[20.1]\Pi_{1/2}$–$X^2\Pi_{3/2}$ ($\nu_o = 20\,106.294$ cm^{-1}) and the $[20.1]\Pi_{1/2}$–$[2.2]A^2\Delta_{3/2}$ ($\nu_o = 17\,882.720$ cm^{-1}) transitions are not observed in emission, and the $[20.1]\Pi_{1/2}$–$[0.25]^2\Sigma^+$ ($\nu_o = 19\,855.042$ cm^{-1}) transition is intense. The nearby $[20.1]\Pi_{1/2}$–$[1.5]^2\Sigma^+$($\nu_o = 18\,532.188$ cm^{-1}) transition is moderately intense and is characterized by headless rotational structure. This new electronic state has not been observed by Chen *et al.* (*15*) when they systematically studied the 17 500–23 000 cm^{-1} spectral region, despite the fact that it is linked to the two lowest electronic states of NiF and that laser-induced experiments should enhance weak transitions. Only the $[20.1]\Pi_{1/2}$–$[0.25]^2\Sigma^+$ ($\nu_o = 19\,855.042$ cm^{-1}) transition has been analyzed. Four of the 6 expected branches have been identified; 256 lines including 9 microwave data of the $[0.25]^2\Sigma^+$ state (*13*) have been fitted. The most striking result is the fact that the rotational parameter B for the upper state is equal to 0.384863 cm^{-1}, a value which is very similar to those of the 5 lowest states (0.386000 cm^{-1} $< B <$ 0.390012 cm^{-1}), while the rotational constants of most of the upper states are in the range 0.378555 to 0.379601 cm^{-1}. This is confirmed by the appearance of the $[20.1]\Pi_{1/2}$–$[1.5]^2\Sigma^+$ ($\nu_o = 18\,532.188$ cm^{-1}) transition. No bandhead was identified because the difference between the rotational constants of upper and lower states is very small. We note that two fine structure parameters, p, and p_J, are necessary, suggesting that the upper state is a $\Pi_{1/2}$ component. Chen *et al.* (*15*) identified a $\Pi_{3/2}$ electronic state located at 20 282 cm^{-1}, and its B parameter is equal to 0.3844 cm^{-1}. As already noted, such large values for the rotational constants compared to those of the three nearby doublet states suggest that these states could be spin–orbit components of a quartet state. In support of this assignment is the fact that if the $[20.1]\Pi_{1/2}$ state was a doublet, we should observe an intense allowed transition to the $[2.2]A^2\Delta_{3/2}$ state in emission, but this transition can be seen only through the sensitive laser-induced fluorescence experiments.

5. The $[20.4]\Omega = 3/2$ State

In increasing order of energy, the next upper electronic state has been reported by Jin *et al.* (*15*) who studied the $[20.4]\ \Omega = 3/2$–$[0.25]^2\Sigma^+$ ($\nu_o = 20\,154.481$ cm^{-1}) transition. It appears that the upper state of this transition has been already studied in a transition located at 17 529.544 cm^{-1} recorded by laser excitation spectroscopy (*10*). More than 220 lines have been recorded and accurate constants, including H and L parameters (caused by perturbations), in the upper state have been determined. In addition low resolution laser-induced fluorescence showed that the $[20.4]\Omega = 3/2$ state is linked to 5 low-lying states, but at that time it had not been possible to include this set of transitions in the energy level diagram of NiF. Comparison with work by Jin *et al.* (*15*) now allows us to identify these transitions. If we consider Fig. 1 of Ref. (*10*), and adding 251 cm^{-1} to the energy of all the identified states there, we observe that the transitions link the upper $[20.4]\Omega = 3/2$ state to the $[0.25]^2\Sigma(\mathrm{v} = 0)$, the $X^2\Pi_{3/2}(\mathrm{v} = 1)$, the $[0.25]^2\Sigma(\mathrm{v} = 1)$, the $[2.2]^2\Delta_{3/2}(\mathrm{v} = 0)$, and the $[2.2]^2\Delta_{3/2}(\mathrm{v} = 1)$ states. The transition rotationally studied in Ref. (*10*) is now identified as the $[20.4]\Omega = 3/2$–$[2.2]^2\Delta_{3/2}(\mathrm{v} = 1)$ transition. The nature of the upper state is determined by the absence of a Q branch and the observation of the $P(J = 2.5)$ and the $R(J = 1.5)$ lines as first lines of the two branches. In the emission spectrum of NiF it has been possible to identify lines of the Q_{ef} and Q_{fe} branches of the weak $[20.4]\Omega = 3/2$–$[0.25]^2\Sigma(\mathrm{v} = 0)$ transition. We have fitted simultaneously all the lines of the two transitions because, as already noted, the resolution of the spectra recorded by Fourier transform spectroscopy or by laser excitation are of the same quality, and microwave data (*13*) for the $[0.25]^2\Sigma$ state have been also included in the fit. Jin *et al.* (*15*) suggest that the $[20.4]\Omega = 3/2$ state is the $\mathrm{v} = 1$ vibrational level of the $[19.7]\Omega = 3/2$ state. This is not confirmed by our analysis for two reasons: first, laser-induced fluorescence experiments show clearly that the upper state is linked to the $\mathrm{v} = 0$ and $\mathrm{v} = 1$ levels of the $[2.2]^2\Delta_{3/2}$ state. This is in agreement with the vibrational constants determined for this state (*10*). In addition we note the closeness of the rotational parameter $B_1 = 0.38509$ cm^{-1} of the $[2.2]^2\Delta_{3/2}(\mathrm{v} = 1)$ state with the value determined for the $[0.83]^2\Delta_{5/2}(\mathrm{v} = 1)$ state, $B_1 = 0.38513$ cm^{-1}, confirming the vibrational assignment of the lower level of the transition located at 17 529.544 cm^{-1}. Second, the evolution of the rotational parameter B with vibrational quantum number v is characterized by an α_e parameter close to 0.003 cm^{-1} for all the studied electronic states (*15, 16*, and Section IV hereafter). Based on the interpretation of Jin *et al.* (*15*) this value would be only $\alpha_e = 0.001$ cm^{-1} for the $[19.7]\Omega = 3/2$ state. Comparison of the line positions of the $[20.4]\Omega = 3/2$–$[0.25]^2\Sigma^+$ transition collected in Table 1 to the values published by Jin *et al.* (*15*) shows that the J-numbering agrees for the lines of the Q_{ef} branch but differs by 3 units in the Q_{fe} branch. Our assignment is also confirmed by microwave data (*13*). However, the symmetry of the $[20.4]\Omega = 3/2$ state is not easy to determine. All the transitions involving this state are very weak, and no more than 87 lines have been observed in emission for the $[20.4]\Omega = 3/2$–$[0.25]^2\Sigma^+$ transition. The two other studied bands, $[20.4]\Omega = 3/2$–$X^2\Pi_{3/2}$ (*15*) and $[20.4]\Omega = 3/2$–$[2.2]A^2\Delta_{3/2}(\mathrm{v} = 1)$ (*10*), have been recorded by laser spectroscopy. Contradictions appear in the usual selection rules if we consider that the upper $[20.4]\Omega = 3/2$ state is linked to the $X^2\Pi_{3/2}$, the $[0.25]^2\Sigma^+$, and the $[2.2]A^2\Delta_{3/2}$ lower states: an upper $[20.4]^2\Pi_{3/2}$ state can be linked to the two first states but not to the third, while a $[20.4]^2\Delta_{3/2}$ state is not expected to be linked to a $^2\Pi_{3/2}$ state and a $^2\Sigma^+$ state.

6. The $[22.9]^2\Pi_{3/2}$ State

The $[22.9]^2\Pi_{3/2}$ state was the first excited state of NiF which was studied by high-resolution spectroscopy (*4*), and it was initially identified as a $^2\Delta_{5/2}$ state. Bai and Hilborn (*11*), however, on the basis of low-resolution laser-induced fluorescence experiments correctly identified this state as a $^2\Pi_{3/2}$ spin–orbit component. The selection rules are satisfied if we consider the intensities of the bands in the emission spectrum, although the $[22.9]^2\Pi_{3/2}$–$X^2\Pi_{3/2}$ ($\nu_o = 22\,955.195$ cm^{-1}) transition is not as intense as expected for an allowed transition. The forbidden $[22.9]^2\Pi_{3/2}$–$[2.2]A^2\Delta_{3/2}$ ($\nu_o = 20\,731.62$ cm^{-1}) transition is only seen in laser-induced fluorescence experiments. The transition located at 22 703.943 cm^{-1} has been identified (*9*) as the $[22.9]^2\Pi_{3/2}$–$[0.25]^2\Sigma^+$ transition and it allowed us to determine the very large spin–rotation parameter of the $[0.25]^2\Sigma^+$ state. The accuracy of the parameters was good enough to allow Tanimoto *et al.* (*13*) to identify the microwave lines of NiF on the basis of a calculated spectrum.

This transition is too weak in the emission spectrum to be analyzed. The line positions determined by dispersed laser-induced fluorescence are not accurate enough to be fitted along with the data collected with Fourier transform spectroscopy, and as a consequence the 540 lines included in the data file belong to the $[22.9]^2\Pi_{3/2}$–$[1.5]B^2\Sigma^+$ (21 381.090 cm^{-1}) and the $[22.9]^2\Pi_{3/2}$–$[0.83]A^2\Delta_{5/2}$ (22 125.719 cm^{-1}) transitions. No fine structure parameters were needed to describe the $[22.9]^2\Pi_{3/2}$ state.

7. The $[23.5]^2\Pi_{1/2}$ State

This state can be identified as the $\Omega = 1/2$ spin–orbit component of a $^2\Pi$ state associated with the $[22.9]^2\Pi_{3/2}$ state to form an inverted $^2\Pi_i$ state. It is linked to the $[2.2]A^2\Delta_{3/2}$ state by an intense transition (21 274.797 cm^{-1}). A weaker transition $[23.5]^2\Pi_{1/2}$–$[1.5]B^2\Sigma^+$ (21 924.265 cm^{-1}) is observed but transitions to the two lowest states are very faint except when laser-enhanced. As expected, no transition is observed in the emission spectrum or in fluorescence experiments connecting to the $[0.83]A^2\Delta_{5/2}$ state. The $[23.5]^2\Pi_{1/2}$–$[2.2]A^2\Delta_{3/2}$ transition is so intense that all 6 possible branches were seen. The Q branches can be followed up to $J = 52.5$. We noted previously that a fine structure splitting was observed in the lower $[2.2]A^2\Delta_{3/2}$ state. To break the strong correlation between fine structure parameters of the two states, we constrained the constants of the lower state to the values derived from the study of the bands linked to the upper $[19.9]\Omega = 5/2$ state. In the $[19.9]\Omega = 5/2$–$[2.2]A^2\Delta_{3/2}$ ($\nu_o = 17\,759.753$ cm^{-1}) transition no lambda doubling was seen in the excited state so the Λ-doubling of the $[2.2]A^2\Delta_{3/2}$ state was well determined. The presence of R, P, and Q branches allowed us to form combination differences, and a residual constant splitting was observed for the e and f levels of the upper state. Thus, a global fit of the

TABLE 3
Observed Line Positions (in cm^{-1}) for the $[18.1]^2\Delta_{5/2}$–$[0.83]A^2\Delta_{5/2}$ and the $[19.9]\Omega = 5/2$–$[0.83]A^2\Delta_{5/2}$ Transitions of ^{58}NiF (1−1), (2−2) and ^{60}NiF (0−0)

	$[18.1]^2\Delta_{5/2}$–$[0.83]A^2\Delta_{5/2}$				$[19.9]\Omega = 5/2$–$[0.83]A^2\Delta_{5/2}$			
	(1–1)		(2–2)		(1–1)		(2–2)	
J	P	R	P	R	P	R	P	R
3.5	17278.478				19153.070			
4.5	17277.624				19152.216			
5.5	17276.759				19151.367			
6.5	17275.904				19150.507			
7.5	17275.027				19149.624			
8.5	17274.112				19148.729			
9.5	17273.186				19147.816			
10.5	17272.248		17276.676		19146.889		19149.807	
11.5	17271.300		17275.722		19145.948		19148.870	
12.5	17270.330		17274.757		19144.966		19147.902	
13.5	17269.321		17273.787		19143.966		19146.957	
14.5			17272.794				19145.948	
15.5	17267.286		17271.769		19141.943		19144.966	
16.5	17266.227				19140.916		19143.966	
17.5	17265.163		17269.679		19139.866		19142.916	
18.5	17264.083		17268.620				19141.847	
19.5	17262.985		17267.540				19140.820	
20.5	17261.872		17266.453	17297.766	19136.583		19139.715	
21.5	17260.719	17293.788	17265.329	17298.134	19135.473		19138.619	
22.5	17259.561	17294.112	17264.187	17298.488	19134.345		19137.505	
23.5	17258.398	17294.462	17263.051	17298.816	19133.199		19136.372	
24.5	17257.218	17294.761	17261.872	17299.148	19132.035		19135.226	
25.5	17256.011	17295.053	17260.719	17299.448	19130.856		19134.062	19172.846
26.5	17254.791	17295.333	17259.512	17299.733			19132.875	19173.146
27.5	17253.552	17295.587		17299.993		19170.496	19131.687	19173.420
28.5	17252.283	17295.829		17300.253		19170.766	19130.455	19173.688
29.5	17251.026	17296.058	17255.796	17300.491		19171.008	19129.226	19173.949
30.5	17249.711	17296.249	17254.544	17300.704	19124.651	19171.231	19127.989	19174.190
31.5	17248.407	17296.433	17253.254	17300.895	19123.363	19171.441	19126.729	19174.418
32.5	17247.081	17296.586	17251.952	17301.079	19122.057	19171.619	19125.445	19174.627
33.5	17245.740	17296.732	17250.646	17301.263	19120.747	19171.802	19124.153	19174.810
34.5	17244.372	17296.859	17249.312	17301.408	19119.418	19171.953	19122.843	19174.966
35.5	17243.005	17296.973	17247.958	17301.538	19118.075	19172.099	19121.523	19175.116
36.5	17241.609	17297.075	17246.597	17301.664	19116.703	19172.231	19120.176	19175.247
37.5	17240.200	17297.139	17245.222	17301.744	19115.327	19172.332	19118.829	19175.384
38.5	17238.769		17243.827		19113.920	19172.437	19117.459	19175.501
39.5	17237.325		17242.410		19112.518	19172.501	19116.062	
40.5	17235.861		17240.980		19111.080		19114.646	
41.5	17234.382		17239.536		19109.623		19113.231	
42.5	17232.897		17238.072		19108.162		19111.797	
43.5	17231.377		17236.600		19106.705		19110.340	
44.5	17229.850		17235.108		19105.212		19108.870	
45.5	17228.303		17233.581		19103.705		19107.390	
46.5	17226.741		17232.068		19102.176		19105.880	
47.5	17225.166		17230.555		19100.632		19104.372	
48.5	17223.570		17228.987		19099.070		19102.820	
49.5	17221.967		17227.418					
50.5	17220.337		17225.822					
51.5	17218.699		17224.233					
52.5	17217.048		17222.610					
53.5	17215.369				19091.070			
54.5	17213.677		17219.328		19089.422			
55.5	17211.977		17217.670		19087.751			
56.5	17210.257		17215.998		19086.080			

TABLE 3—*Continued*

	$[18.1]^2\Delta_{5/2}$–$[0.83]A^2\Delta_{5/2}$			$[19.9]\Omega = 5/2$–$[0.83]A^2\Delta_{5/2}$			
	(1–1)	(2–2)		(1–1)		(2–2)	
J	R	P	R	P	R	P	R
57.5	17208.520			19084.386			
58.5	17206.774			19082.678			
59.5			17210.886	19080.956			
60.5			17209.145	19079.226			
61.5			17207.387	19077.472			
62.5			17205.648	19075.705			
63.5			17203.864	19073.924			
64.5			17202.080	19072.125			
65.5			17200.280	19070.312			
66.5				19068.481			
67.5				19066.636			

	$[18.1]^2\Delta_{5/2}$–$[0.83]A^2\Delta_{5/2}$		$[19.9]\Omega = 5/2$–$[0.83]A^2\Delta_{5/2}$	
	^{60}NiF (0–0)			
J	P	R	P	R
7.5				19159.654
8.5				19160.247
9.5		17284.832		19160.829
10.5		17285.400		19161.399
11.5		17285.924		19161.941
12.5	17266.911	17286.447	19142.916	19162.492
13.5	17265.908	17286.954	19141.943	19162.992
14.5	17264.871	17287.423	19140.916	19163.464
15.5	17263.846	17287.903	19139.866	19163.985
16.5	17262.781	17288.344	19138.829	19164.414
17.5	17261.712	17288.780	19137.784	19164.857
18.5	17260.620	17289.177	19136.706	19165.273
19.5	17259.512	17289.557	19135.605	19165.693
20.5	17258.398	17289.948	19134.482	19166.058
21.5	17257.218	17290.290	19133.350	19166.432
22.5	17256.071	17290.616	19132.194	19166.802
23.5	17254.891	17290.935	19131.025	19167.126
24.5	17253.711	17291.228	19129.843	19167.414
25.5	17252.476	17291.508	19128.646	19167.725
26.5	17251.226	17291.785	19127.427	19168.012
27.5	17249.976	17292.015	19126.194	19168.254
28.5	17248.706	17292.215	19124.943	
29.5	17247.419		19123.674	
30.5	17246.113		19122.395	19168.944
31.5	17244.773	17292.771	19121.085	
32.5	17243.460	17292.937	19119.765	
33.5	17242.093	17293.086	19118.432	19169.455
34.5	17240.718	17293.207	19117.080	19169.601
35.5	17239.329		19115.715	19169.743
36.5	17237.899		19114.308	19169.817
37.5	17236.476		19112.906	19169.926
38.5	17235.004		19111.454	
39.5	17233.553		19110.034	
40.5	17232.068		19108.582	
41.5	17230.555		19107.112	
42.5	17229.049		19105.623	
43.5	17227.515		19104.130	
44.5	17225.967		19102.610	
45.5	17224.392		19101.071	
46.5	17222.810		19099.518	
47.5			19097.957	
48.5	17219.591		19096.377	
49.5	17217.960		19094.774	
50.5	17216.302		19093.162	
51.5	17214.644		19091.536	
52.5	17212.951		19089.893	
53.5	17211.252		19088.235	
54.5	17209.531		19086.550	
55.5	17207.799		19084.856	
56.5	17206.035		19083.148	
57.5	17204.278		19081.422	
58.5	17202.500		19079.687	
59.5	17200.684		19077.929	
60.5	17198.873		19076.157	
61.5	17197.043		19074.381	
62.5	17195.219		19072.573	
63.5	17193.315		19070.764	
64.5	17191.472		19068.943	
65.5	17189.555		19067.084	
66.5			19065.230	
67.5			19063.362	
68.5			19061.463	
69.5			19059.564	
70.5			19057.658	
71.5			19055.731	
72.5			19053.783	
73.5			19051.834	
74.5			19049.849	
75.5			19047.863	
76.5			19045.844	
77.5			19043.837	
78.5			19041.820	
79.5			19039.775	
80.5			19037.715	

TABLE 4

Origins of the 1–1, 2–2 Bands of ^{58}NiF and of the 0–0 Bands for the $[18.1]^2\Delta_{5/2}$–$[0.83]A^2\Delta_{5/2}$ and the $[19.9]\Omega = 5/2$–$[0.83]A^2\Delta_{5/2}$ Transitions (All Uncertainties Are 1σ)

Transition	v′–v″	ν_{origin} (cm^{-1})
^{58}NiF		
$[18.1]^2\Delta_{5/2}$–$[0.83]A^2\Delta_{5/2}$	1–1	17281.232(22)
	2–2	17285.554(26)
$[19.9]\Omega = 5/2$–$[0.83]A^2\Delta_{5/2}$	1–1	19155.820(20)
	2–2	19158.654(23)
^{60}NiF		
$[18.1]^2\Delta_{5/2}$–$[0.83]A^2\Delta_{5/2}$	0–0	17277.868(25)
$[19.9]\Omega = 5/2$–$[0.83]A^2\Delta_{5/2}$	0–0	19153.824(23)

lines was unsatisfactory unless we added a phenomenological constant parameter $a = -0.0791$ cm^{-1} to T_0 ($T_0 \pm a$) to allow the e and f levels of the upper $[23.5]^2\Pi_{1/2}$ state to have slightly different origins.

IV. STUDY OF SOME VIBRATIONAL AND ISOTOPOMERIC BANDS

In addition to the study of 0–0 bands of the main ^{58}NiF isotopomer, it has been possible to identify some 1–1 and 2–2 bands and two 0–0 bands of the ^{60}NiF isotopomer. In each case the $[0.83]A^2\Delta_{5/2}$ state is common to the studied transitions. The bands are generally weak and as a consequence the derived parameters are not very accurate, especially D. The experimental data are listed in Table 3, the origins of the bands in Table 4, and the derived parameters in Table 5. For the upper states the rotational parameters are in agreement with those determined by Jin *et al.* (*16*).

TABLE 5

Molecular Constants (in cm^{-1}) for the $[19.9]\Omega = 5/2$, $[18.1]^2\Delta_{5/2}$, and $[0.83]A^2\Delta_{3/2}$ States for v = 0, 1, and 2 and Derived Equilibrium Constants (All Uncertainties are 1σ) for NiF

	v	B_v	$D_v \times 10^{-7}$	B_e	α_e
$[19.9]\Omega = 5/2$	2	0.373692(60)	5.40(25)	0.380966(80)	0.002925(65)
	1	0.376503(54)	4.85(23)		
	0	0.3795417(13)	4.902(22)		
	0^a	0.376399(11)	4.87(11)		
$[18.1]^2\Delta_{5/2}$	2	0.373258(58)	4.92(20)	0.380632(80)	0.002964(64)
	1	0.376111(55)	4.85(22)		
	0	0.3791866(18)	4.988(10)		
	0^a	0.376042(10)	4.95(10)		
$[0.83]A^2\Delta_{3/2}$	2	0.381948(55)	5.40(25)	0.390172(95)	0.003306(77)
	1	0.385130(54)	5.30(21)		
	0	0.3885599(23)	5.427(10)		
	0^a	0.385326(10)	5.35(10)		

^{a} Constants for v = 0 of ^{60}NiF isotopomer.

V. DISCUSSION

The object of our discussion is not to provide an interpretation of the electronic structure of NiF, but to point out some characteristic features and problems, which will have to be solved.

Six new electronic transitions have been analyzed in our work. These analyses confirmed the previous (*4–10*) description of the 5 electronic states lying in the first 2000 cm^{-1} in the energy level diagram. If we compare the 2 isovalent molecules NiF and NiCl (*17, 19, 20*), the same low-lying electronic states are observed and the ground state is, in both cases, a $^2\Pi_{3/2}$ spin–orbit component, but the order of the other states is somewhat different. In the present work, as well as for NiCl (*20*), we took advantage of the accurate data provided by Tanimoto *et al.* (*13*) for the 2 lowest states ($X^2\Pi_{3/2}$ and $[0.25]^2\Sigma^+$) to improve the quality of the parameters. Rather than fixing the parameters of these states to the values determined by Tanimoto *et al.* (*13*) we included the original microwave data in the fits. This results in some small differences (Table 1) between our constants and those of Tanimoto *et al.* (*13*). These discrepancies are real because in a first step we fitted the microwave data alone and the derived parameters lay within one standard deviation of the published values. However, for example, if we consider the $[19.7]\Omega = 3/2$–$[0.25]^2\Sigma^+$ ($\nu_o = 19\,467.723$ cm^{-1}) transition, we observe a difference of 3×10^{-7} cm^{-1} in γ_D between our results and those reported in Ref. (*13*). This difference results in a small change in the calculated $J = 17.5$–16.5 transition, which is the highest J value observed in the microwave experiments (*13*). However, the highest J transition observed in the present work is $J = 75.5$, for which the line positions are shifted by 0.13 cm^{-1}, which is about 10 times larger than the error in our measurements. Correlation between the parameters may also be responsible for part of the shifts in the parameters. Nevertheless, the presence of the microwave data in the fits resulted in a significant improvement in the accuracy of the parameters when compared to the previous studies (*4–10*). For example, the fine structure of the $[2.2]A^2\Delta_{3/2}$ state is determined for the first time. The determination of a Λ-doubling parameter p is not expected in a $^2\Delta_{3/2}$ spin–orbit component but rather for a $^2\Pi_{1/2}$ state (*21*). This parameter is 30 to 50 times smaller than any of the other values of p determined for other states of NiF. Taking into account the selection rules, it appears to be difficult to change the assignment of the symmetry of this state. The origin of this p parameter is thus likely to be in interactions with close-lying doublet or quartet states (*12*).

Our combined fits showed some additional unexpected parameters that appear because of perturbations. For example, a splitting of the lines proportional to J^3 is observed in the P and R branches of the $[18.1]^2\Delta_{5/2}$–$[0.83]A^2\Delta_{5/2}$ ($\nu_o = 17\,277.897$ cm^{-1}) transition that can be attributed to the upper $[18.1]^2\Delta_{5/2}$ state. A phenomenological constant, a, was needed in the upper $[23.5]\ ^2\Pi_{1/2}$ state to allow the e and f levels to have a different origin. We observe that the $[18.1]^2\Delta_{5/2}$ and $[23.5]^2\Pi_{1/2}$ states are not located in congested parts of the energy level diagram, but unobserved close-lying electronic states are possible.

The 19 700–20 500 cm^{-1} range in the energy level diagram includes 5 spin–orbit components. In some cases it has been possible to assign the symmetry and/or the multiplicity of the states. Two types of evidence were used for these assignments: the selection rules and the size of the rotational constant. Considering the theoretical predictions of the states given by Carette *et al.* (*12*), we expect to find four states, $^2\Sigma^+$, $^4\Pi$, $^2\Pi$, and $^4\Sigma^+$ states in the range 18 900–21 500 cm^{-1}. In addition, two spin–orbit components of a $^2\Delta_i$ state are calculated to be at 17 464 cm^{-1} and 17 946 cm^{-1}. The lower energy spin component can be assigned as the $[18.1]^2\Delta_{5/2}$ state, but the upper spin component ($^2\Delta_{3/2}$) is not yet observed. In the absence of a second predicted $^2\Delta_i$ state, it appears difficult to identify the $[19.9]\Omega = 5/2$ state as a $^2\Delta_{5/2}$ state despite the fact that transitions involving this state fulfill the expected selections rules.

No confusion is possible with $v' > 0$ vibrational levels of any excited state because vibrational constants have been estimated for the $[18.1]^2\Delta_{5/2}$, $[19.7]\Omega = 3/2$ and $[19.9]\Omega = 5/2$ electronic states by Focsa *et al.* (*10*). Jin *et al.* (*15*) suggested that the $[20.4]\Omega = 3/2$ state is the $v' = 1$ vibrational level of the $[19.7]\Omega = 3/2$ state. Such an assignment, however, is not possible because the $[19.7]\Omega = 3/2$ state has $\omega_e' = 642.08$ cm^{-1} (*10*) while the measured interval is 687.6 cm^{-1}. Jin *et al.* (*15*) suggested that the difference between the two intervals ($\omega_e = 642.08$ cm^{-1} (*10*) and their value, $\omega_e = 687.6$ cm^{-1}) is due to a repulsive interaction of two close-lying states. This is in contradiction with our spectrum, recorded by laser excitation spectroscopy, which finds the 1–1 bandhead of the $[19.7]\Omega = 3/2$–$[2.2]A^2\Delta_{3/2}$ transition at 17 509.02 cm^{-1}, which is the expected position in the absence of any interaction. This could explain the fact that the expected and calculated shifts between the two isotopomers, ^{58}NiF and ^{60}NiF, are not in agreement in Jin *et al.* (*15*).

In a recent paper Jin *et al.* (*16*) published an extensive vibrational analysis of most of the excited states of NiF. We note that they do not observe the $[20.1]\Pi_{1/2}$ state. The vibrational constants are not in very good agreement with the previous values (*10*). The vibrational constants, ω_e, are in some cases 15 cm^{-1} larger than those in Ref. (*10*), in which the vibrational structure has been determined from experimental data that includes bandheads from 5 upper states and 3 lower states. The discrepancies in the values originate primarily because Focsa *et al.* (*10*) used heads while Jin *et al.* (*16*) used origins to determine the vibrational parameters.

Although it is not a general rule, for some molecules such as GeF and InF (*22*), when states of different multiplicity are close-lying, their rotational constants are significantly different. In the case of NiF, Table 1 shows that rotational constants of two upper states are close to 0.385 cm^{-1}, while for all other states the B values are smaller than 0.379 cm^{-1}. This difference can be taken as evidence that both quartet and doublets states are present in the 19 700–20 500 cm^{-1} energy range.

VI. CONCLUSION

The NiF emission was produced by a DC discharge of heated NiF_2 powder in a 1-meter-long alumina tube. Comparison with microwave discharge emission (*17*) shows that rotational lines are wider (*23*) but fewer argon atomic lines are emitted. When combined with a Fourier transform spectrometer, this source is very efficient thanks to its stability and longevity. The quality of the recorded spectra provided an improved set of parameters for most of the known states of NiF. The use of pure rotational data (*13*), when possible, was of great help in breaking the correlation between parameters of the upper and lower states. The low-lying doublet states are now very well determined and can be used to identify other new electronic states. This should be of great help for further studies in spectral regions in which laser experiments are difficult to perform such as the UV work of Gopal *et al.* (*24*).

The presence of excited states with significantly different rotational constants suggests that both doublet and quartet states are involved in the observed transitions. Up to now the nature of the excited states of NiF is not well determined, and further theoretical and experimental work is needed to understand the energy level pattern. Recent studies on the isovalent NiCl molecule (*17, 19, 20, 25*) should allow useful comparisons.

ACKNOWLEDGMENTS

We thank the Natural Sciences and Engineering Research Council of Canada for financial support. The Centre d'Etudes et de Recherches Lasers et Applications is supported by the Ministère Chargé de la Recherche, the Région Nord-Pas de Calais, and the Fond Européen de Développement Economique des Régions.

REFERENCES

1. V. G. Krishnamurty, *Indian J. Phys.* **27,** 354–358 (1953).
2. R. Gopal and M. M. Joshi, *Curr. Sci.* **50,** 530–531 (1981).
3. R. Gopal, L. K. Singh, and M. M. Joshi, *Indian J. Phys. B* **55,** 507–509 (1981).
4. B. Pinchemel, Y. Lefebvre, and J. Schamps, *J. Mol. Spectrosc.* **75,** 29–35 (1979).
5. B. Pinchemel, *J. Phys. B* **14,** 2569–2573 (1981).
6. C. Dufour, I. Hikmet, and B. Pinchemel, *J. Mol. Spectrosc.* **158,** 392–398 (1993).
7. C. Dufour, I. Hikmet, and B. Pinchemel, *J. Mol. Spectrosc.* **165,** 398–405 (1994).
8. A. Boudou, C. Dufour, and B. Pinchemel, *J. Mol. Spectrosc.* **168,** 477–482 (1994).
9. C. Dufour and B. Pinchemel, *J. Mol. Spectrosc.* **173,** 70–78 (1995).
10. C. Focsa, C. Dufour, and B. Pinchemel, *J. Mol. Spectrosc.* **182,** 65–71 (1997).
11. J. Bai and R. C. Hilborn, *Chem. Phys. Lett.* **128,** 133–136 (1986).
12. P. Carette, C. Dufour, and B. Pinchemel, *J. Mol. Spectrosc.* **161,** 323–335 (1993).
13. M. Tanimoto, T. Sakamaki, and T. Okabayashi, *J. Mol. Spectrosc.* **207,** 66–69 (2001).
14. Y. Chen, J. Jin, C. Hu, X. Yang, X. Ma, and C. Chen, *J. Mol. Spectrosc.* **203,** 37–40 (2000).
15. J. Jin, Y. Chen, C. Hu, X. Yang, Q. Ran, and C. Chen, *J. Mol. Spectrosc.* **208,** 18–24 (2001).

16. J. Jin, Q. Ran, X. Yang, Y. Chen, and C. Chen, *J. Phys. Chem. A* **105,** 11177–11182 (2001).
17. T. Hirao, C. Dufour, B. Pinchemel, and P. F. Bernath, *J. Mol. Spectrosc.* **202,** 53–38 (2000).
18. G. Norlén, *Phys. Scr.* **8,** 249–268 (1973).
19. A. Poclet, Y. Krouti, T. Hirao, B. Pinchemel, and P. F. Bernath, *J. Mol. Spectrosc.* **204,** 125–132 (2000).
20. Y. Krouti, A. Poclet, T. Hirao, B. Pinchemel, and P. F. Bernath, *J. Mol. Spectrosc.* **210,** 41–50 (2001).
21. G. Herzberg, "Spectra of Diatomic Molecules." Van Nostrand, New York, 1950.
22. K. P. Huber and G. Herzberg, "Constants of Diatomic Molecules." Van Nostrand–Reinhold, New York, 1979.
23. T. Hirao, K. Tereszchuk, and P. F. Bernath, to be published.
24. R. Gopal, K. N. Uttam, and M. M. Joshi, *Indian J. Phys. B* **64,** 468–474 (1990).
25. E. Yamazaki, T. Okabayashi, and M. Tanimoto, *Astrophys. J. Lett.* **551,** L199–L201 (2000).